Signal Design and Processing Techniques for WSR-88D Ambiguity Resolution

The CLEAN-AP Filter

National Severe Storms Laboratory Report

prepared by: **Sebastian Torres, David Warde, and Dusan Zrnic**

Part 15
January 2012

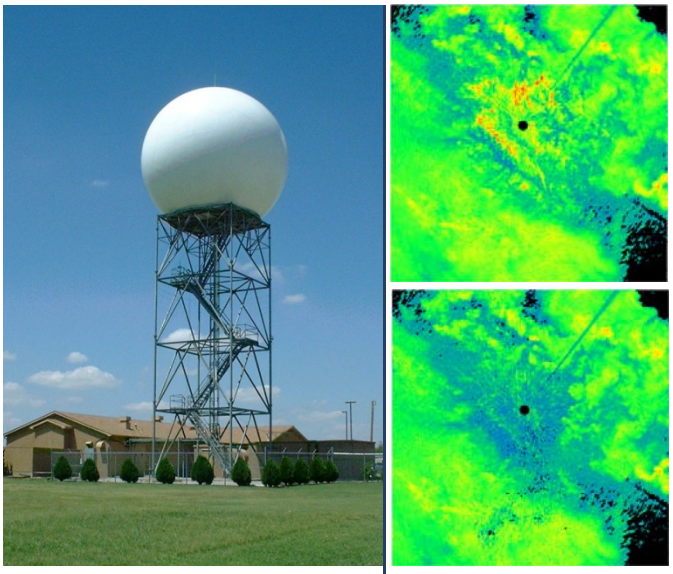

National Oceanic and Atmospheric Administration
National Severe Storms Laboratory

SIGNAL DESIGN AND PROCESSING TECHNIQUES FOR WSR-88D AMBIGUITY RESOLUTION

Part 15: The CLEAN-AP Filter

National Severe Storms Laboratory Report

prepared by: Sebastián Torres, David Warde, and Dusan Zrnić

January 2012

NOAA, National Severe Storms Laboratory
120 David L. Boren Blvd., Norman, Oklahoma 73072

SIGNAL DESIGN AND PROCESSING TECHNIQUES FOR WSR-88D AMBIGUITY RESOLUTION

Part 15: The CLEAN-AP Filter

Contents

SIGNAL DESIGN AND PROCESSING TECHNIQUES FOR WSR-88D AMBIGUITY RESOLUTION

Part 15: The CLEAN-AP Filter

1. Introduction

The Radar Operations Center (ROC) of the National Weather Service (NWS) has funded the National Severe Storms Laboratory (NSSL) to address data quality improvements for the WSR-88D. This is the fifteenth report in the series that deals with data quality techniques for the WSR-88D (other relevant reports are listed at the end); it documents NSSL accomplishments in FY11.

This report focuses on the CLEAN-AP filter and the work done to request official approval from the NEXRAD Technical Advisory Committee, which was granted. The CLEAN-AP filter was developed for the National Weather Radar Testbed Phased Array Radar (NWRT PAR), but is currently recommended as a complete ground-clutter mitigation technique for future upgrades of the WSR-88D. CLEAN-AP combines automatic detection and filtering capabilities so that seamless integration with other functions in the signal-processing pipeline is possible. The performance of the CLEAN-AP filter was extensively quantified using simulations within the framework outlined by the NEXRAD Technical Requirements (NTR) in our previous report (NSSL Report 14). The filter was shown to meet NTR and exceed the already superior performance of GMAP. Qualitative comparisons with the currently operational clutter mitigation scheme revealed the potential for improved data quality with less user intervention.

This report also includes two appendices. Appendix A contains comments on the report by Baron Services (2011) concerning accuracy of Z_{DR} calibration. Appendix B includes a list of relevant publications.

Once again, the work performed in FY11 exceeded the allocated budget; hence, a part of it had to be done on other NOAA funds.

2. The CLEAN-AP Filter

The CLutter Environment ANalysis using Adaptive Processing filter (CLEAN-AP© 2009, Board of Regents of the University of Oklahoma; Warde and Torres 2009) was developed by NSSL in the spring of 2008 with the goal of providing effective ground-clutter mitigation for the National Weather Radar Testbed Phased Array Radar (NWRT PAR) in Norman, OK. As such, a major milestone in the development of CLEAN-AP has been its real-time implementation on the NWRT PAR, which took place in the fall of 2008. Although CLEAN-AP was developed for and implemented on a PAR, it is important to note that it is perfectly suited for implementation on conventional radars such as the WSR-88D. In fact, in March 2011, the NEXRAD Technical Advisory Committee (TAC) officially recommended an engineering evaluation of CLEAN-AP through its implementation on the WSR-88D Radar Data Acquisition (RDA) subsystem.

As documented in NSSL Report 14 (Torres et al. 2010), CLEAN-AP is a novel real-time, automatic, integrated technique for ground clutter detection and filtering that produces data with better quality while meeting NEXRAD technical requirements. These attractive characteristics of CLEAN-AP were validated by comprehensive performance analyses using simulations and qualitative assessments using a data cases collected with WSR-88D radars (KEMX in Tucson, AZ; KTLX in Oklahoma City, OK; KABX in Albuquerque, NM; and the ROC's KCRI radar in Norman, OK).

In the spring of 2010, CLEAN-AP was extended to include suppression control via a clutter model and to work on polarimetric radars. This new version of the algorithms was tested on the same data cases mentioned above and also on polarimetric data collected

with the KOUN (S band) and OU Prime (C band) radars, both in Norman, OK. Currently, we are working on extending CLEAN-AP to staggered-PRT and alternating-dual-polarization waveforms.

In this report, we document the salient properties of the CLEAN-AP filter that make it uniquely suited for operational implementation on the NEXRAD network.

2.1. Ground Clutter Mitigation on the NEXRAD Network

Ground clutter mitigation (detection and filtering) continues to be a major concern for operational, ground-based, Doppler weather radars. In fact, the need for a complete and automatic ground clutter mitigation technique was recognized by the NEXRAD TAC as one of the strategic directions for future improvements (Snow and Scott 2003). In their report, the TAC stated that investments should be made to "*…produce the best quality data possible from the WSR-88D throughout the remainder of its service life*." Further, they recognized the need that *"...quality control/assurance be applied automatically"* and that *"...signal processing could be improved to almost completely mitigate ground clutter..."*

Ground clutter mitigation consists of two functions: detection and filtering. An effective detection algorithm should apply (or bypass) the ground clutter filter when ground clutter is present (or absent) in the received radar signal. Upon detecting the presence of ground clutter contamination, a ground clutter filter should be applied to provide effective ground clutter suppression with minimum disturbance of the desired weather signal. Thus, the goal of the two functions is to work collectively to mitigate ground clutter and provide high-quality estimates of meteorological variables. To accomplish this goal, the

detection algorithm should not miss a ground-clutter contaminated gate; otherwise, the non-filterednon-filtered ground clutter results in hot spots. Just as important, the ground clutter filter should not overly suppress ground clutter when the detection algorithm falsely identifies a clutter-contaminated gate. Such false detections create irregularities or partial and even complete loss of the meteorological-variable estimates.

As of RDA software build 11, ground clutter mitigation at the RDA consists of the Clutter Mitigation Decision (CMD) detection algorithm (Hubbert et al. 2009) and the Gaussian Model Adaptive Processing (GMAP) filter (Siggia and Passarelli 2004). Although these represent a significant improvement over legacy techniques (i.e., a static clutter map and a 5th-order elliptic filter), the ROC has received field complaints regarding

(a) **false detections along zero isodop** where GMAP is applied on non-contaminated gates and reflectivity is biased low ("signal loss"),

(b) **missed detections for multiple clutter sources** where GMAP is not applied on contaminated gates and reflectivity is biased high ("hot spots"), and

(c) **spatial irregularities in data fields** where GMAP is applied or not applied on "patches" of data causing obvious and distracting spatial discontinuities (see Fig. 1). The main reason for these artifacts is the spatial map "growing" process that was implemented to minimize missed detections, but it results in excessive filtering (NSSL Report 14).

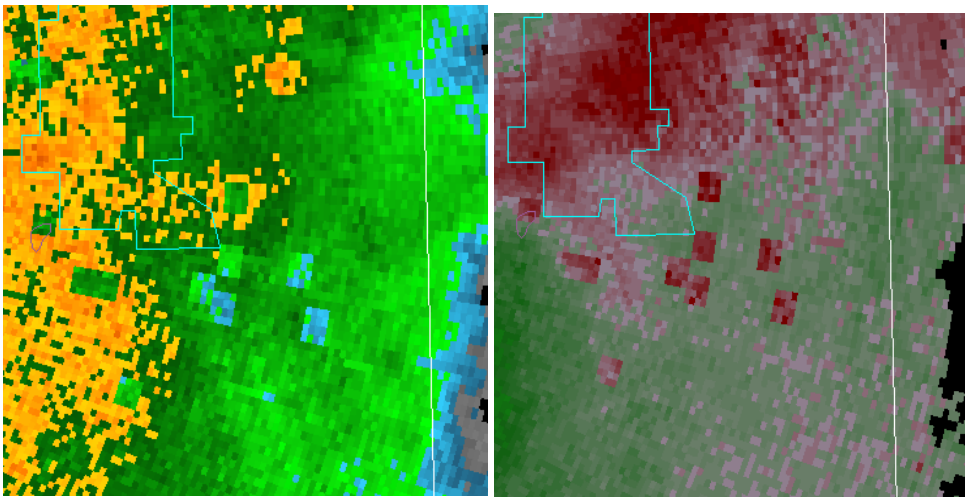

Fig. 1. Example of spatial irregularities in reflectivity (right) and velocity(left) fields on RDA build 11. Data was collected with the KTLX radar on 23 Aug 2010. The images are courtesy of NWS's Weather Dicision Training Branch.

2.1. CLEAN-AP Filter Characteristics

The CLEAN-AP filter is a spectral ground clutter filter (GCF) capable of mitigating the adverse effects of ground-clutter contamination while preserving the quality of the meteorological-variable estimates. This 'smart' filter performs real-time detection and suppression of ground-clutter returns in dynamic atmospheric environments.

The CLEAN-AP filter is automatic; that is, it performs real-time ground-clutter detection with no need for user intervention or clutter maps. In fact, clutter maps become obsolete with CLEAN-AP since the detection component of it runs on all bins. However, this does not mean that filtering will occur on all bins. This is similar to the concept of operations for CMD and GMAP, where CMD runs on all bins, but GMAP is applied only when CMD detects clutter contamination. If users need to be aware of bins with filtered ground-clutter contamination, a CLEAN-AP clutter-map equivalent can be produced based on the amount of power removed or the filter's notch width.

The CLEAN-AP filter produces data with better quality. It is well known that data windows make spectral processing possible by containing the spectral leakage inherent in the discrete-time Fourier transform (DFT) of aperiodic signals (Harris 1978). The larger the dynamic range or power difference between the different signals in the Doppler spectrum, the more aggressive (or tapered) the data window that is needed to contain spectral leakage. However, aggressively tapered data windows use less of the information from the end samples in the dwell; this increases the variance of estimates derived from the spectrum. Hence, it is important to select the least tapered data window needed for a particular situation. Compared to the current approach that employs a Blackman data window when GMAP is applied, CLEAN-AP adaptively selects a data window to find a good compromise between clutter suppression and data quality. Thus, as the clutter contamination goes from weak to strong, CLEAN-AP uses more tapered data windows.

The CLEAN-AP filter meets NEXRAD technical requirements for ground-clutter suppression. In fact, CLEAN-AP achieves larger suppression than GMAP and can meet technical requirements for reflectivity estimates with as few as 9 samples.

The CLEAN-AP filter is an integrated approach (see Fig. 2); that is, it incorporates ground-clutter detection and filtering into a single algorithm. Further, CLEAN-AP operates on a single bin at a time, which is the preferable way of processing signals at the RDA. Single-bin algorithms lead to better data partitioning on multi-processor systems, and minimize compatibility issues with other existing or planned signal-processing techniques.

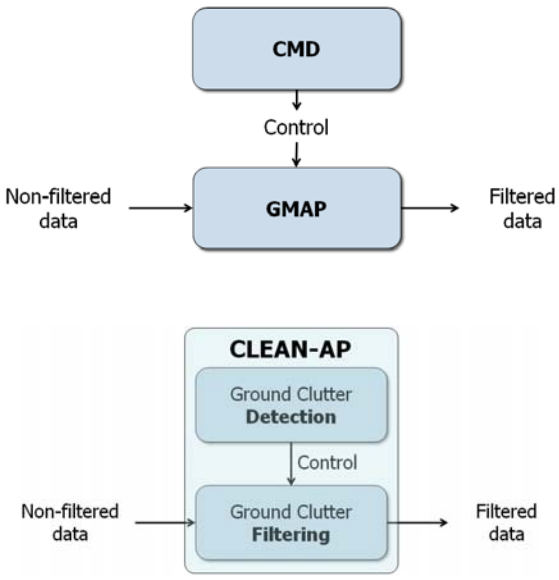

Fig. 2. Current (top) and proposed (bottom) clutter mitigation at the WSR-88D RDA. In the current implementation, CMD performs clutter detection while GMAP performs clutter filtering. In the proposed implementation CLEAN-AP performs both functions in an integrated algorithm.

The CLEAN-AP filter "sets the stage" for further spectral processing. With the advent of modern signal processors and the drastic increase in computational power, spectral processing has become the domain of choice for artifact removal on operational weather radars. This is because, compared to time-domain filters, frequency-domain filters are more attractive for several reasons: ideal filters can be perfectly realized, artifacts can be readily identified, and filter compensation (e.g., the reconstruction of the weather signal in the filter's notch) is possible. Typically, frequency-domain filters operate on the Doppler spectrum obtained using the periodogram estimator. Conversely, CLEAN-AP operates on the autocorrelation spectral density (ASD) which is immune to biases from the circular convolution inherent to periodogram-based estimates and, more importantly, preserves the phase information.

The CLEAN-AP filter has been running on the National Weather Radar Testbed (NWRT) Phased-Array Radar (PAR) since September of 2008, and its performance has been qualitatively evaluated by meteorologists and forecasters who participate in the yearly Phased-Array Radar Innovative Sensing Experiments (PARISE).

In summary, CLEAN-AP is a very advantageous alternative solution for clutter mitigation on the NEXRAD network. CLEAN-AP addresses all of the existing operational issues, improves on the current performance, and is compatible with operational techniques and future upgrades such as dual polarization, SZ-2, staggered PRT, and range oversampling.

2.2. CLEAN-AP Filter Description

In a nutshell, the CLEAN-AP filter operates on the ASD domain and consists of four basic steps: (1) data-window selection, (2) identification of spectral components with ground-clutter contamination, (3) removal of contaminated spectral components, and (4) reconstruction of the filtered spectrum.

The lag-1 autocorrelation spectral density, S_1, is at the core of CLEAN-AP. It is defined as the cross-spectrum of time-shifted signals, where the time shift is the pulse repetition time (T_s). That is,

$$S_1(k) = F_0^*(k)F_1(k),\ k = 0,\ldots,M-2\,, \tag{3.1}$$

where F_l is the discrete Fourier transform (DFT) of the received complex voltages $V_l(m)$, $m = l, l+1, \ldots, M-1-l$. A graphical depiction of this process is shown in Fig. 3.

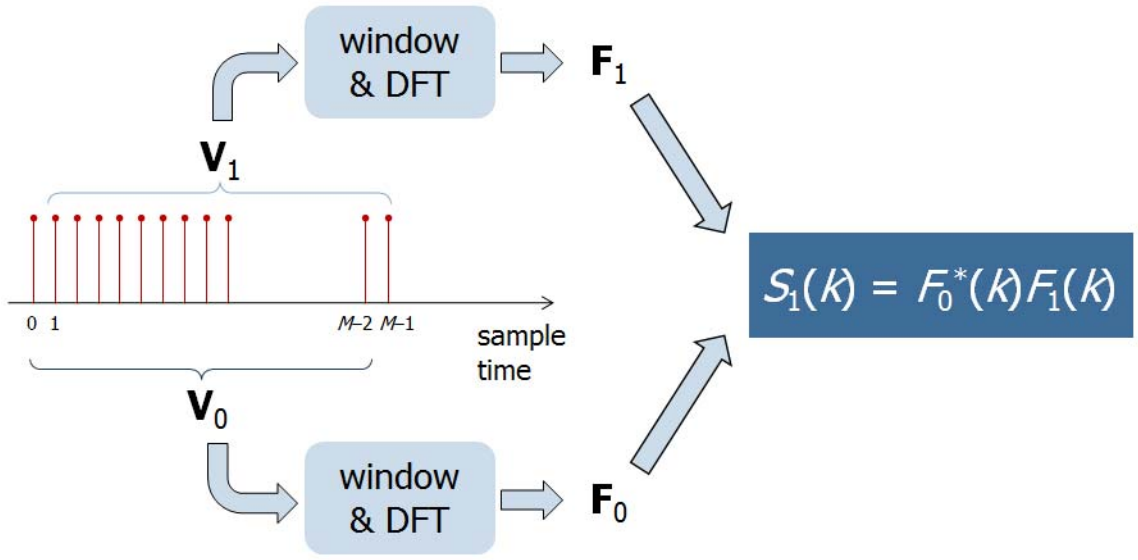

Fig. 3. Lag-1 ASD computation. *M* is the number of samples in the dwell. The window is chosen adaptively to get the desired clutter suppression with the best quality of estimates.

It can be shown mathematically that the sum of the lag-1 ASD coefficients over the Nyquist co-interval is proportional to the lag-1 autocorrelation, thus the name autocorrelation *spectral density*. Computing the ASD requires two DFTs, making it computationally more complex than the power spectral density (PSD), which requires only one DFT. However, it will be shown later that the ASD is better suited than the PSD for spectral processing of weather signals.

For periodic signals with period $(M-1)T_s$, the lag-1 ASD is simply the PSD, S, with a (trivial) linear phase. That is,

$$S_1(k) = F_0^*(k)F_0(k)e^{j2\pi k/(M-1)} = S(k)e^{j\alpha k} . \tag{3.2}$$

However, weather signals are typically not periodic and the phase of the ASD actually conveys useful information. Not unlike the PSD, the ASD is susceptible to spectral leakage both in magnitude and phase; and spectral leakage in the phase of the *measured*

ASD is the basis for ground-clutter detection in CLEAN-AP. Fig. 4 shows a cartoon of true vs. measured ASD for ground-clutter and weather signals. Note that the spectral leakage in the phase of the measured ASD causes the phases around the mean Doppler velocity to be biased towards that central value. For example, for the ground-clutter case, the mean Doppler velocity is zero and the phases around zero velocity are biased towards zero phase. On the other hand, for the weather-signal case, the mean Doppler velocity is v (away from zero) and the phases around v are biased towards $\pi v/v_a$, where v_a is the Nyquist velocity. In comparing these two cases, note that if the power gradient about the mean Doppler velocity is large, the phase biases are large as well.

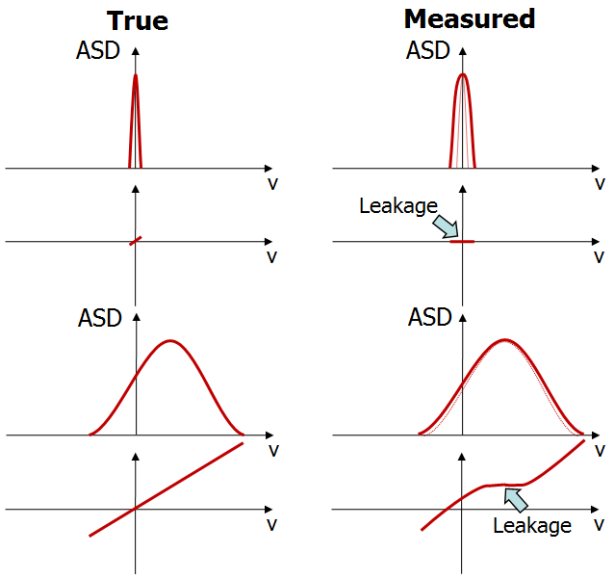

Fig. 4. True (left) and measured (right) ASDs for a ground-clutter (top) and weather (bottom) signals. Note the biases in the phase of the measured ASD due to spectral leakage.

As shown in Fig. 5, the CLEAN-AP filter operates by identifying and removing the near-zero phase components of the lag-1 ASD *in the vicinity of zero Doppler velocity* and

reconstructing the weather signal spectrum over the filter's notch. The first step adaptively determines the filter's notch, which depends on the clutter-to-signal ratio (CSR) and the data window used. The second step is similar to other spectral filters; here, the reconstruction is done using independent linear interpolations of magnitude and phase over the notch.

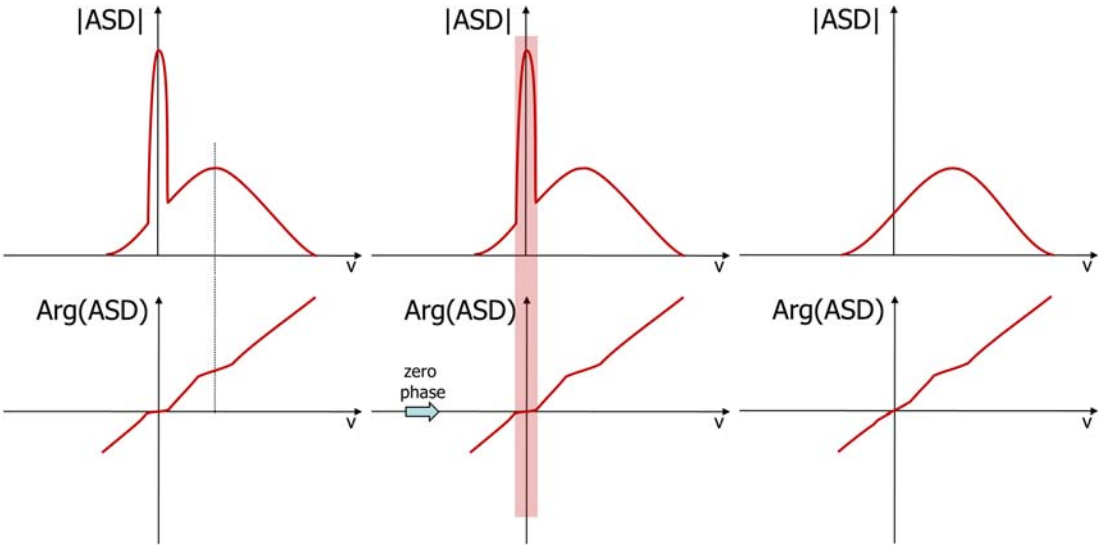

Fig. 5. (left) Measured lag-1 ASD of a weather signal with ground-clutter contamination. (middle) Identification of spectral components with near-zero ASD phase around zero Doppler velocity. (rigth) Filtered lag-1 ASD from which the meteorological variables can be estimated.

As mentioned before, tapered data windows are effective in containing spectral leakage. However, to maximize the quality of estimates derived from the spectrum, the degree of tapering has to be tailored to the dynamic range of the signals under analysis. Fig. 6 shows the true lag-1 ASDs for a ground-clutter signal and its measured counterparts using rectangular and Blackman data windows. The rectangular window with no tapering exhibits a power spectrum with first sidelobe levels that are 13 dB down from the main lobe. Obviously, these are not low enough to contain the spectral leakage of the ground-clutter signal, and the phase of the ASD becomes identically zero. The heavily tapered

Blackman window has a power spectrum with first sidelobe levels 58 dB down from the main lobe. These are sufficient to control the spectral leakage at the price of broadening the measured spectrum. Thus, in this case, only a few coefficients around zero Doppler velocity are biased towards zero phase, and the rest follow the predicted linear behavior.

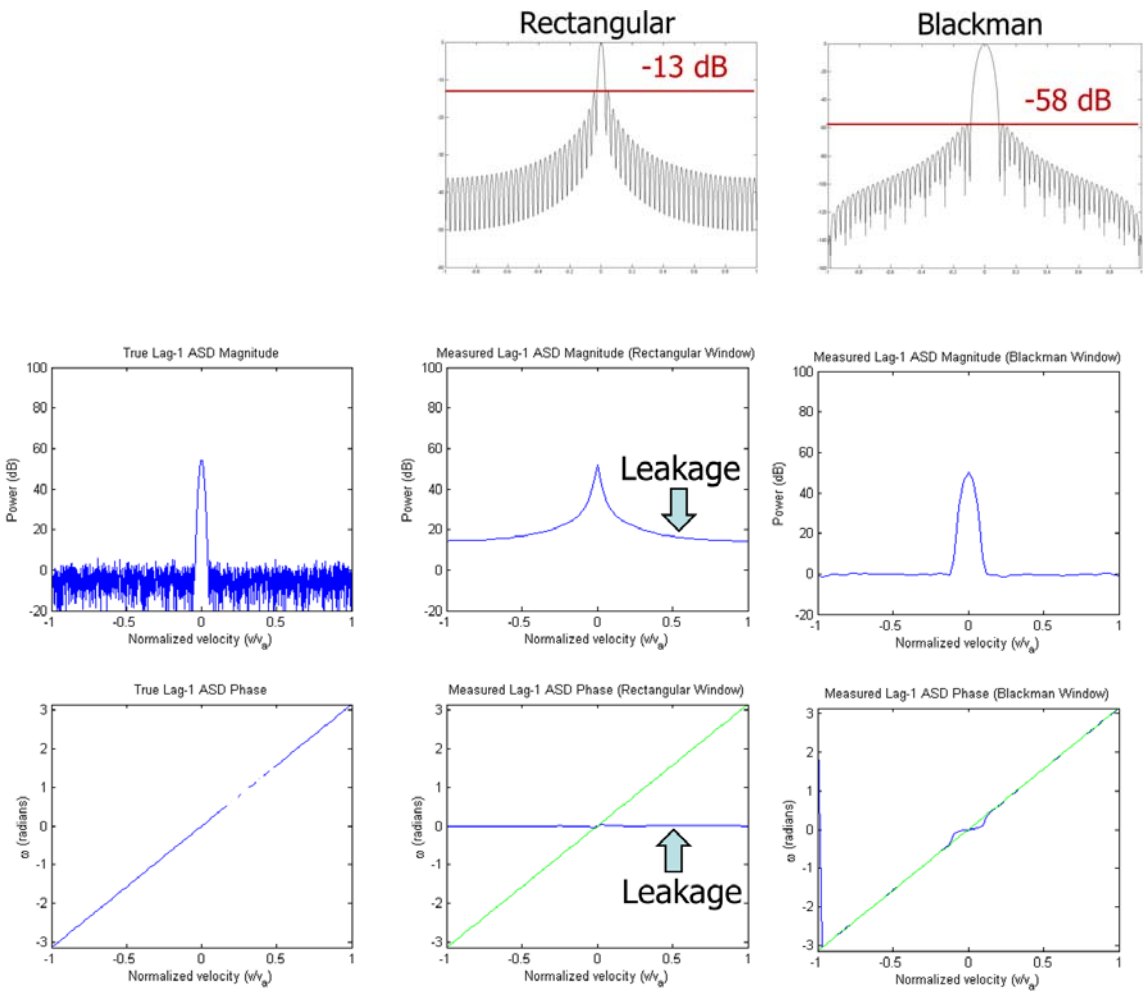

Fig. 6. True (left) and measured lag-1 ASD using the rectangular (middle) and Blackman (right) windows. The top row shows the power spectra of the data windows, the middle and bottom rows are the magnitude and phase of the ASD, respectively.

Fig. 7 shows a histogram of the data window selected by CLEAN-AP as a function of the CSR. The *y*-axis corresponds to the different windows (rectangular, von Hann, Blackman, and Blackmn-Nutall) and the colors represent the frequency of selection as a

percentage. Compared to GMAP, which uses the Blackman window regardless of the CSR, CLEAN-AP realizes the required suppression with less aggressive data windows (and lower variance of estimates) for CSRs below about 20 dB, and is able to achieve higher suppression levels for CSRs above about 40 dB.

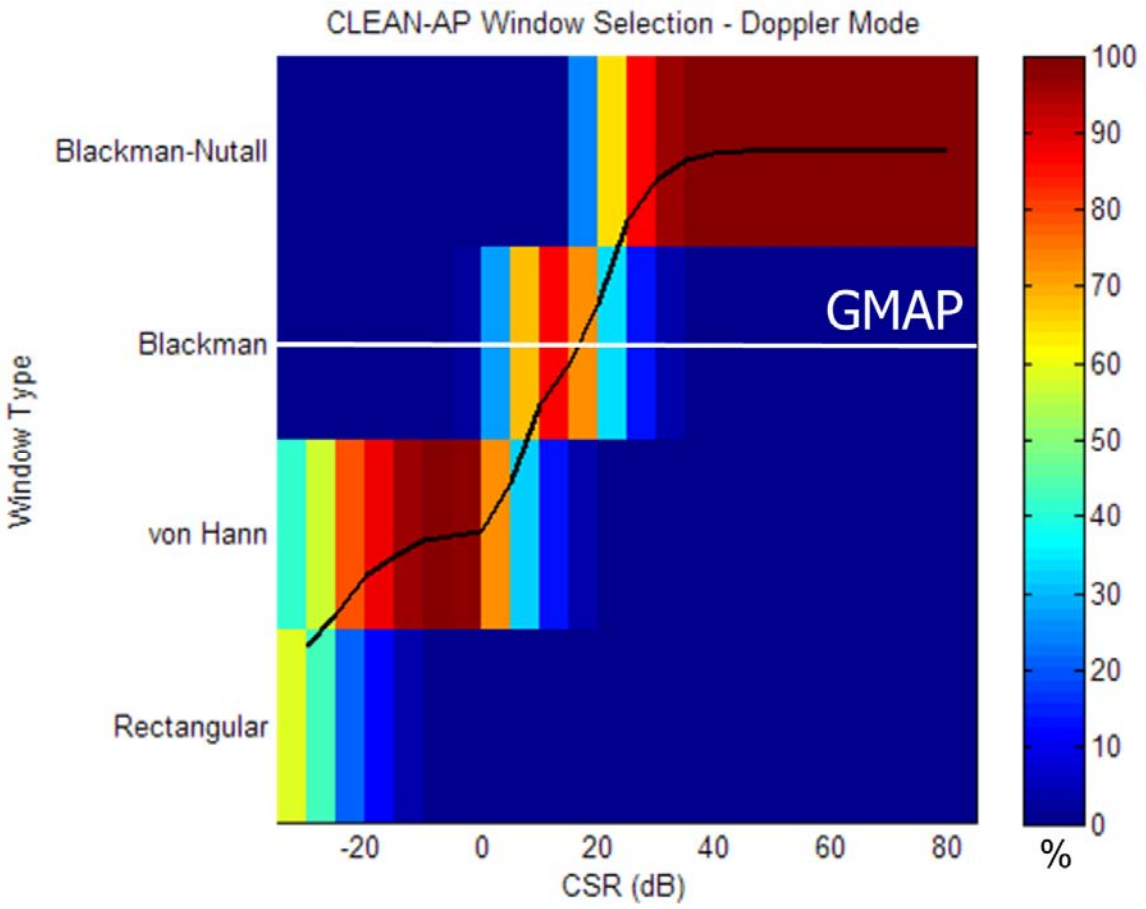

Fig. 7. Frequency of window-type selection as a function of the CSR. CLEAN-AP chooses the best window for a given CSR among rectangular, von Hann, Blackman, and Blackman-Nutall, whereas GMAP uses the Blackman window all the time. The black solid line represents the mean behavior as a function of the CSR.

One of the latest improvements to CLEAN-AP was the addition of a clutter model to allow for automatic phase threshold adjustments for different sampling and processing conditions (i.e., changes in PRT, number of samples, and data window). This clutter model is analogous to GMAP's clutter model; the filter's suppression can be controlled

via a single parameter; namely, the *expected* spectrum width of ground clutter. This parameter can be optimized for different clutter environments with the goal of achieving the required clutter suppression levels while maintaining small biases along the zero isodop.

Like GMAP, CLEAN-AP's notch width is adaptable; however, CLEAN-AP uses both the magnitude and phase of the lag-1 ASD and the clutter model to determine an optimum notch width setting. Fig 8 compares the ground-clutter filter's notch width selection for GMAP and CLEAN-AP. GMAP relies only on the PSD (i.e., magnitude only) to determine the notch width and imposes empirical lower and upper limits on it. Thus, at low CSRs, GMAP's notch width is wider than needed resulting in larger biases along the zero isodop. At high CSRs, GMAP's notch width is not as wide as it should be, and its suppression does not achieve the required levels. In contrast, CLEAN-AP's notch width is allowed to span the entire sample range, from 1 sample at low CSRs to the total number of samples at very high CSRs. However, in extreme contamination cases (CSRs larger than about 50 dB) where the filter's notch width needs to be larger than about 50% of the Nyquist co-interval (i.e., a normalized notch width larger than 0.5), a censoring scheme is implemented to flag the bin as unrecoverable (similarly to the dB-for-dB censoring in the WSR-88D).

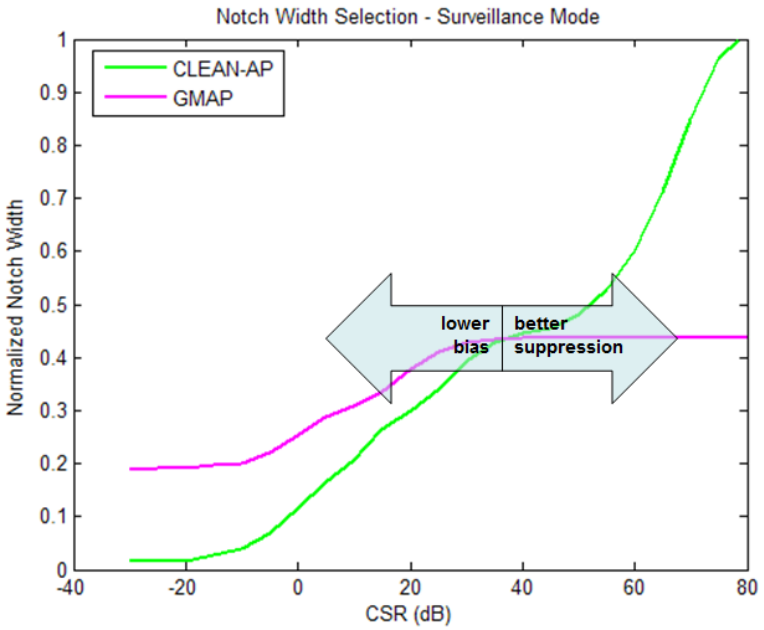

Fig. 8. GMAP and CLEAN-AP notch-width selection as a function of the CSR. GMAP uses the magnitude of the spectrum only and imposes lower and upper limits on the notch width. Thus, at low CSRs, it uses a wider than needed notch width resulting in larger biases. At high CSRs, it uses a narrower than needed notch width resulting in under suppression. CLEAN-AP allows the notch width to span the entire range.

Fig. 9 shows an example of CLEAN-AP filtering on the lag-1 ASD of real data collected with the KOUN radar in Norman, OK using VCP 12 with a PRT of 1 ms and 40 samples per radial. In this case, the strong clutter contamination (high CNR) led to the selection of the Blackman-Nutall window. The lag-1 ASD phase biases (from spectral leakage) around zero Doppler velocity were used to identify the components with clutter contamination; in this case, 7 spectral components (highlighted in red in Fig. 9). These were removed and the magnitude and phase of the ASD were linearly interpolated (dotted lines in Fig. 9) using the uncontaminated spectral coefficients on either side of the filter's notch. In this case, the filter achieved a clutter suppression of ~48 dB.

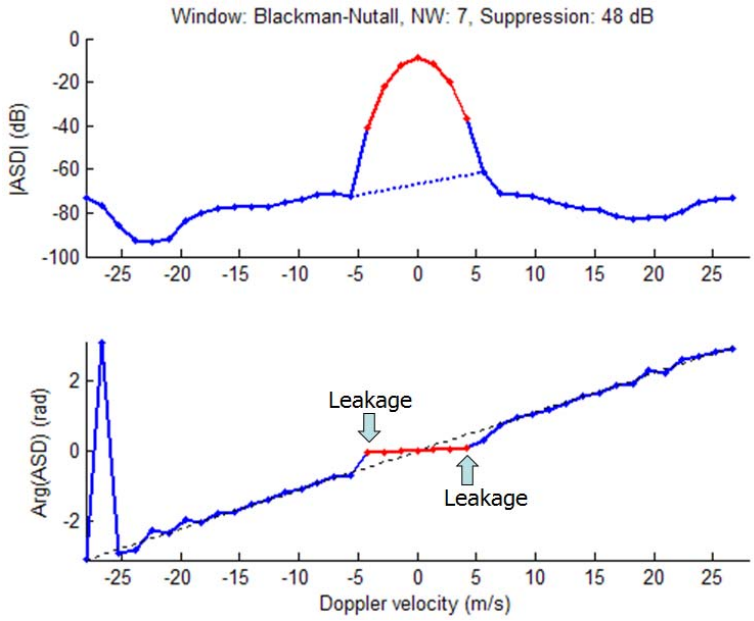

Fig. 9. Example of CLEAN-AP performance on the lag-1 ASD of real data collected with the KOUN radar with T_s = 1 ms and M = 40. In this case, CLEAN-AP's notch width is 7 samples and the filter achieves a suppression of ~48 dB with the Blackman-Nutall window.

It was mentioned before that computation of the ASD requires two DFTs and that the CLEAN-AP filter is an "all-bins" approach, which could be a concern for real-time implementation on signal-processing systems with limited capacity. We believe that the proposed solution will fit in the current WSR-88D signal processor without any additional processing requirements or hardware upgrades. The reason for this is twofold. On one hand, CLEAN-AP requires less processing time than GMAP. Although the ASD requires almost twice the number of computations than the PSD, GMAP uses a recursive spectral reconstruction technique after filtering that more than makes up for the additional FFT in CLEAN-AP. On the other hand, even though GMAP is not an "all-bins" approach, some sites have routinely used it as such. Thus, there is anecdotal evidence that the WSR-88D signal processor is able to run an "all-bins" GMAP, which is computationally more expensive than CLEAN-AP.

In terms of implementation, CLEAN-AP is also simpler than the current approach. Fig. 10 shows a block diagram of the CMD and GMAP implementation (ORDA software build 11) compared to the proposed implementation of CLEAN-AP. Whereas CMD splits its functionality between the RVP-8 and RCP-8 subsystems and requires both a filtered and non-filtered stream, CLEAN-AP is confined to the RVP-8 as an integrated, gate-by-gate implementation of clutter detection and filtering. As mentioned before, we strongly believe that this is the preferred way of doing signal processing in the RDA.

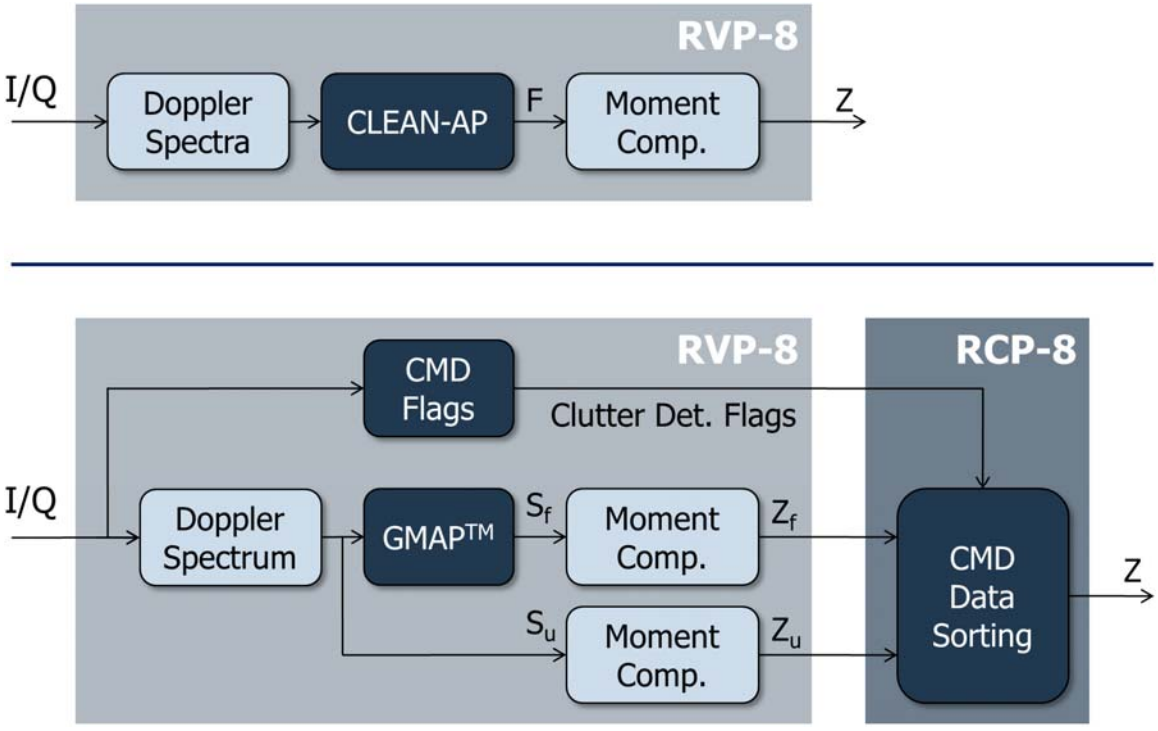

Fig. 10. Block diagrams for the ORDA build 11 CMD/GMAP and the proposed CLEAN-AP implementations. Whereas the CMD/GMAP implementation is split between the RVP-8 and RCP-8 computers and requires filtered and non-filtered streams, the CLEAN-AP implementation is integrated, operates on a single range gate at a time, and is confined to the RVP-8.

2.3. Comparison between CLEAN-AP and CMD/GMAP

In this section, we compare the performance of the proposed ground-clutter mitigation approach, CLEAN-AP, with the "current" implementation, CMD and GMAP (herein denoted as CMD/GMAP). CMD was introduced in ORDA software build 11 and, unfortunately, was retired in build 12 (the dual polarization build). It is expected that CMD will be completely revamped and re-introduced in build 13 to include the dual-polarization variables and several other improvements. Although improvements to CMD's performance are expected, implementation details were unknown at the time of this writing. Thus, our comparisons in this report are based on the CMD implementation in ORDA software build 11.

Whereas CLEAN-AP is an "all-bins" approach and is spatially consistent, CMD/GMAP is an "on/off" approach which leads to spatial inconsistencies (Fig. 1). Further, in the ORDA implementation, these spatial inconsistencies are amplified because the CMD clutter map is dilated such that isolated detections are artificially propagated to neighboring bins. This may force the application of GMAP on bins that may not have ground-clutter contamination. Thus, as will be shown later, the main limitation of CMD/GMAP comes from the fact that *CMD's false detections are heavily penalized by GMAP's suboptimal filtering performance*. That is, the price to pay for CMD's detection mistakes is large biases of meteorological-variable estimates.

In terms of performance evaluation, the main distinction between CLEAN-AP and CMD/GMAP comes from the single-bin vs. multiple-bin concepts of operation, respectively. Whereas CLEAN-AP can be fully characterized with simulations,

simulations can only be used to characterize GMAP's *filtering* performance (Ice et al. 2004a, 2004b); the full CMD/GMAP performance must be characterized using real data with realistic range profiles.

To understand the approach adopted to compare the performances of CLEAN-AP and CMD/GMAP, consider the following two scenarios for CMD: the zero-isodop and the weak-clutter cases.

i) Zero-isodop case

Ground-clutter detection in CMD is based on a fuzzy-logic scheme with three inputs: coherent phase alignment (CPA), spin of reflectivity (SPIN), and texture of reflectivity (TDBZ). The membership functions that define the interest values for these variables are shown in Fig. 11 (from Hubbert et al. 2009).

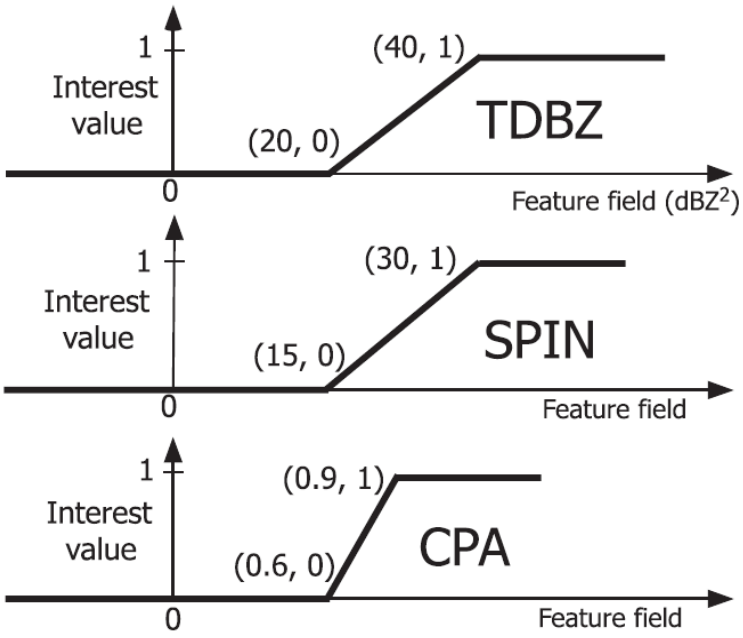

Fig. 11. [extracted from Hubbert et al. 2009] CMD membership functions and their break points.

A simple analysis can be conducted if we (conservatively) assume that a detection is triggered based only on CPA (i.e., with no contributions from TDBZ or SPIN). Because CPA receives a weight of 1.01/2.01 = 0.502, a CPA interest value of 1 (a CPA value larger than 0.9) is enough to trigger a detection. That is, even with very small interest values of TDBZ and SPIN, the output of the fuzzy-logic engine with a CPA value larger than 0.9 is 0.505. This output is larger than the detection threshold (0.5) and triggers the application of GMAP. Thus, the question is: *which meteorological conditions lead to a CPA value larger than 0.9 and a guaranteed detection?* Fig. 12 shows the probability of having a CPA value larger than 0.9 (i.e., a guaranteed CMD detection) for a simulated weather signal with zero Doppler velocity and varying spectrum widths between 0.1 and 2 m/s. Specifically, for a weather signal with zero Doppler velocity and a narrow spectrum width of 0.5 m/s, CMD makes a false detection about 30% of the time. Further, it was shown in Fig. 3.5 of NSSL Report 14 (Torres et al. 2010) that under these conditions, GMAP introduces a reflectivity bias of ~23 dB whereas reflectivity biases from CLEAN-AP are only ~5 dB. However, note that reflectivity biases from CLEAN-AP occur 100% of the time under the stated conditions whereas CMD/GMAP introduces no bias 70% of the time and a much larger bias of ~23 dB the other 30%. Even if these biases only occur a small fraction of the time, forecasters using the base data do not have the luxury of seeing "average performance" or of waiting for the next volume scan hoping that no false detections will occur. Unfortunately, the reality is that one bad image is enough to reduce the forcasters' confidence in the base data. So, as mentioned before, a false

CMD detection along the zero isodop is severely penalized by the poor performance of GMAP, and this has a significant impact on users.

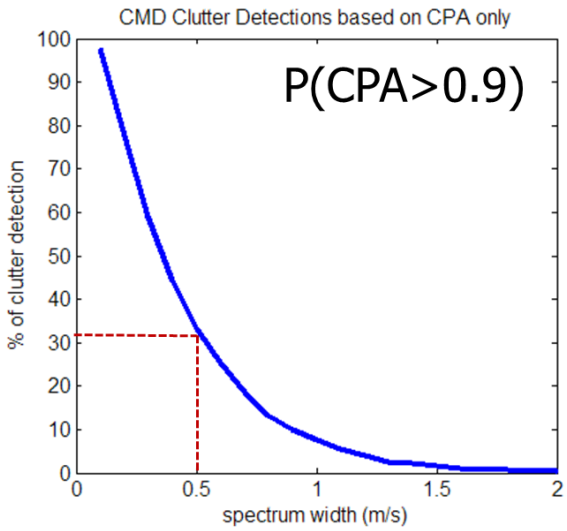

Fig. 12. Probability of having a CPA value larger than 0.9 for a simulated weather signal with zero Doppler velocity and spectrum widths between 0.1 and 2 m/s.

ii) Weak-clutter case

Based on published data (Hubbert et al. 2009), CMD misses a detection more than 50% of the time for CSRs less than -8 dB. Although at this level of clutter contamination, meteorological-variable biases from non-filtered data are small, a missed detection of a bin with only clutter can be operationally significant in terms of overlaid echo recovery. That is, assume for example that an overlaid echo situation exists between a strong weather signal and a weak ground-clutter signal. Further, consider the case in which the SNRs are 8 dB and 4 dB for the strong and weak echoes, respectively (the word "signal" here is used loosely and refers to the weather or the clutter signal). In this scenario, using the legacy WSR-88D range-unfolding

algorithm, the parameters of the strong overlaid echo can be recovered only if the ground clutter in the weak echo is detected and removed. Otherwise, the weak echo power is such that the strong echo power does not exceed the typical operational overlaid threshold of 5 dB. Thus, a missed detection in this scenario would result in the parameters of the strong echo being obscured by the "purple haze."

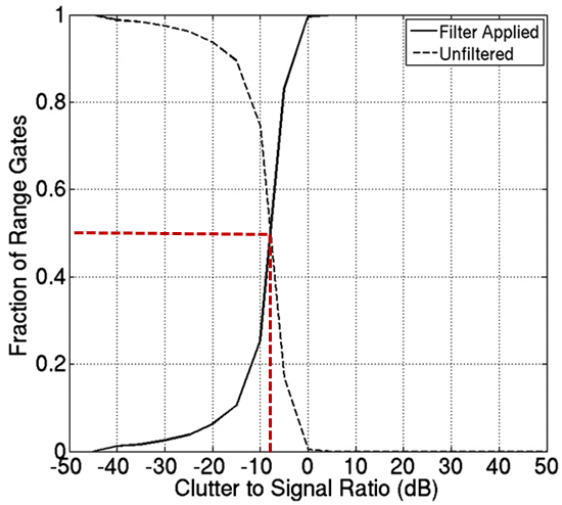

Fig. 13. [extracted from Hubbert et al. 2009] CMD's probability of detection (solid line) as a function of the CSR. For a CSR < -8dB, the probability of detection is 50%. That is, half of the time, weak-clutter contamination remains undetected.

As stated before, a direct performance comparison between CLEAN-AP and CMD/GMAP is not straightforward: whereas CMD/GMAP can be naturally broken up into detection and filtering functions, CLEAN-AP is integrated and such functional separation is not feasible. Because CMD does not operate on a single bin at a time, real data are needed to perform a full comparison. However, if a CMD detection is assumed (based on published results, this is true 100% of the time for CSRs larger than 0 dB), simulations can be used whether there is clutter contamination or not. In this case the

problem reduces to comparing CLEAN-AP vs. GMAP. Thus, the suppression of the filter, and the bias and variance of filtered estimates can be systematically evaluated. CLEAN-AP's performance along the zero-isodop can be fully quantified using simulations, but real data are needed to do the same with CMD/GMAP. Along the same lines, missed detections (e.g., spatial discontinuities, "hot spots", or weak-clutter contamination) can only be evaluated using real data since the performance of the CMD/GMAP combo depends heavily on CMD's behavior.

In the following section, comparisons between CLEAN-AP and CMD/GMAP performance are consider for 5 cases, the first two are analyzed using simulations, and the last three require the use of real data cases.

1. **Typical case with clutter contamination**: For CSR levels above 0 dB, where CMD makes a detection and there is clutter contamination, the clutter suppression performance of CLEAN-AP vs. GMAP using simulations is analyzed under the conditions stated in the WSR-88D System Specifications.
2. **Zero isodop losses**: When CMD makes a detection and there is no clutter contamination, the biases in the meteorological-variable estimates when a non-contaminated weather signal is filtered using simulations are analyzed under the conditions stated in the WSR-88D System Specifications.
3. **Missed CMD detections**: When CMD does not make a detection and there is clutter contamination, examples of CLEAN-AP and CMD/GMAP performance are contrasted using real data from KEMX in Tucson, AZ.
4. **Typical case with no clutter contamination**: When CMD does not make a detection and there is no clutter contamination, examples of CLEAN-AP and

CMD/GMAP performance are contrasted using real-data from KCRI in Norman, OK.

5. **CMD/GMAP spatial discontinuities**: When CMD toggles detections in neighboring gates, examples of CLEAN-AP and CMD/GMAP performance are contrasted using real-data from KCRI in Norman, OK.

2.4. CLEAN-AP Performance Analysis

The CLEAN-AP filter clutter mitigation performance was reported by Warde and Torres (2009) using a MATLAB implementation and signal simulations. Additionally, Warde and Torres (2010) used recorded time-series data from WSR-88D operational sites to qualitatively assess the detection performance of the CLEAN-AP filter. These results were also documented in detail in NSSL Report 14 (Torres et al. 2010). The results from the simulations and the real data show that the CLEAN-AP filter meets and in most cases exceeds the WSR-88D requirements for both ground clutter detection and filtering. Unlike previous analyses, where the implementation of CLEAN-AP did not include a clutter model to control the filter's notch width, in this report, the most up-to-date CLEAN-AP implementation is evaluated. The clutter model provides optimal filter control based on the data window used in the FFT processes, the radar wavelength and setup parameters (PRT and dwell time), and the expected ground clutter spectrum width (seed width) (Ice et al. 2004a). The WSR-88D system currently uses a seed width of 0.4 m/s; whereas, a seed width of 0.3 m/s for CLEAN-AP filter is recommended.

2.4.1. *WSR-88D Ground Clutter Suppression Requirements*

The WSR-88D System Specifications (SS) 2810000H dated 25 April 2008, chapter 3.7.2.7 (Ground Clutter Suppression) provides bias and standard deviation requirements for the application of a filter for a signal at 20 dB signal-to-noise ratio (SNR) with a weather spectrum width (σ_v) of 4 m/s. Clutter model A of the WSR-88D SS provides for a zero-mean normally distributed clutter model and is most relevant for this ground clutter filter evaluation. Although not specified in the WSR-88D SS, a 0.28 m/s clutter spectrum width is used which is in line with the expected clutter spectrum width of 0.1 m/s when accounting for spectrum broadening due to the antenna motion. Additionally, 0.28 m/s clutter spectrum width provides ready comparison with earlier filter evaluations conducted for the WSR-88D system at the Radar Operation Center (e.g. Sirmans 1992, Ice et al. 2004a). When applied, the filter is required to provide a clutter suppression capability of 30 dB in the reflectivity channel and selectable clutter-suppression levels of 20 dB for low, 28 dB for medium, and 50 dB for high clutter suppression in the Doppler channel (velocity and spectrum width). Here, clutter suppression is defined as the ratio of the input power to the output power after application of the clutter filter. The biases on the meteorological-variable estimates caused by the application of the filter are assessed with a signal-to-clutter ratio (SCR) of 30 dB. In the bias assessment, a low clutter level with a high signal level is used so that the prominent contributor to the bias is associated with the filter performance and not the clutter residue. An additional allowance in estimate biases is provided in the WSR-88D SS when clutter residue is present in the output signal. That is, the system allows for a reflectivity bias of 1 dB for an output SCR

of 10 dB, velocity bias of 1 m/s for an output SCR of 11 dB and spectrum width bias of 1 m/s for an output SCR of 15 dB.

The filtered reflectivity bias requirement is assessed with a weather signal at 0 m/s and is dependent on the spectrum width of the weather as shown in table 1 (reproduced from the WSR-88D SS). As can be seen in table 1, the bias in reflectivity is expected to increase as the weather spectrum width becomes small compared to the notch width of the clutter filter. The bias in reflectivity is due to portions of the weather signal coincident with the notch width of the filter centered at 0 m/s. When the weather signal is completely contained within the notch width of the filter, the parameters of the weather signal are likely to be unrecoverable (i.e., they are severely biased).

Table 1, WSR-88D Filtered Reflectivity Bias Requirements

Weather Spectrum Width (m/s)	Maximum Bias of Reflectivity (dB)
1	10
2	2
≥3	1

Filtered Doppler moments have a bias requirement of less than 2 m/s over a range of usable velocities as a function of the notch width selection as shown in table 2 (reproduced from the WSR-88D SS). This requirement is for an IIR filter with selectable notch widths. The WSR-88D system no longer uses an IIR filter; however, filtered velocity and spectrum width biases and standard deviations can be assessed to ensure 2 m/s is not exceeded for all usable velocities above those minimums stated on the left side of table 2 (when the filter provides the clutter suppression level listed on the right side of the table).

Table 2, WSR-88D Usable Filtered Velocity Requirement

Notch Width Selection	Minimum Usable Velocity (m/s)	Clutter Suppression (dB)
Low	2	20
Medium	3	28
High	4	50

2.4.2. *Ground Clutter Suppression*

Referring to Fig. 13, the reported detection performance of CMD is near 100% at ~0 dB CSR; accordingly, the GMAP filter is always applied above this CSR level. Above ~0 dB CSR, the statistical performance of CLEAN-AP and CMD/GMAP (i.e., GMAP filter always applied) provides an insight into operational implications of each ground clutter mitigation technique. Figs. 14, 15, and 16 show a top view of 3-D histograms of power bias (dB) for CLEAN-AP (left) and GMAP (right) as a function of CSR (dB). The percentage of 1700 realizations of each power bias per CSR are shown in color (dark blue = 0% to red = 50%). Ground clutter suppression is seen in these figures as the point where the power bias departs from zero and becomes positively biased (i.e., more ground clutter present in the output signal). Both filters easily surpass the WSR-88D SS (red dotted lines) for ground clutter suppression. However, notice that the CLEAN-AP filter provides over 60 dB of ground clutter suppression in all modes used on the WSR-88D system; whereas, the GMAP filter provides poor ground clutter suppression above 50 dB, especially in the Surveillance mode.

The variance of power estimates can readily be seen in Figs. 14, 15, and 16 for different weather modes. Observe how the power bias is more localized around 0 dB when using

the CLEAN-AP filter compared to using the GMAP filter. The adaptive ground clutter suppression performance of the CLEAN-AP filter is readily seen to reduce the variance as less ground clutter contamination is detected (i.e., at lower CSR levels). The sharper color transitions (progressing from blues toward reds) around the 0 dB bias line in the CLEAN-AP panels of Figs. 14, 15, and 16 indicate a lower variance in the power estimates which translates into more precise reflectivity estimates.

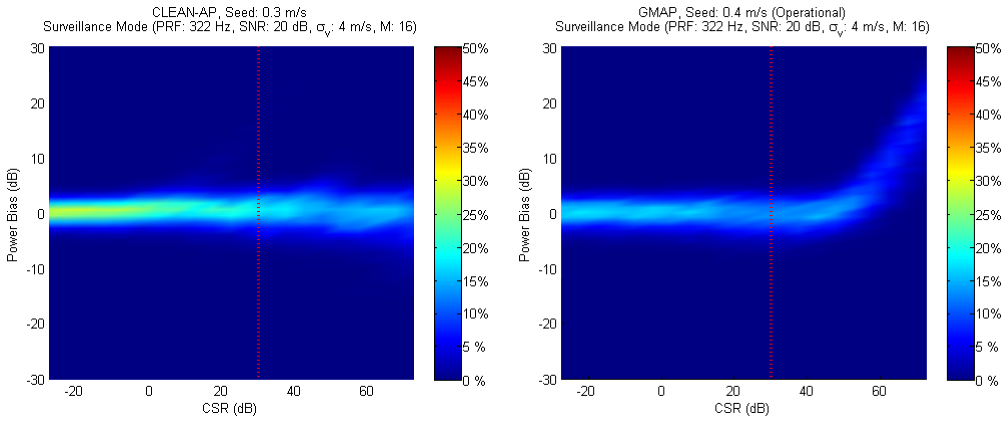

Fig. 14. CLEAN-AP (left) and GMAP (right) power bias performance for Surveillance Mode (PRF 322 Hz, SNR 20dB, spectrum width of 4 m/s, 16 samples).

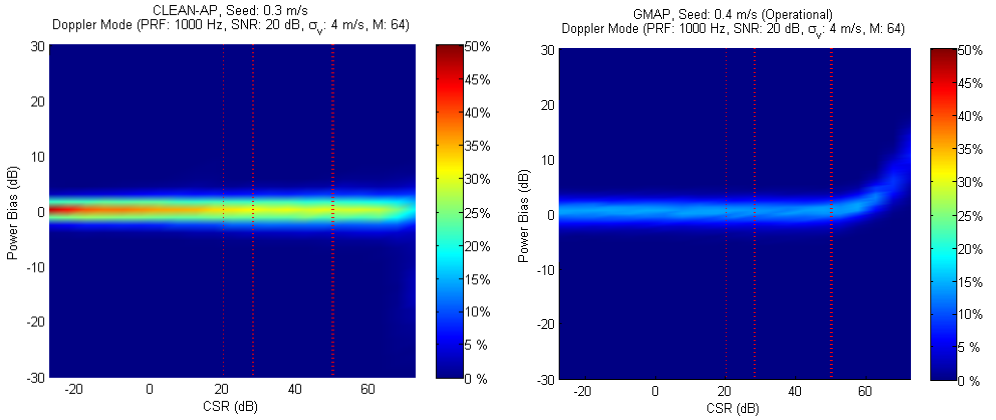

Fig. 15. CLEAN-AP (left) and GMAP (right) power bias for Doppler Mode (PRF 1000 Hz, SNR 20dB, spectrum width of 4 m/s, 64 samples).

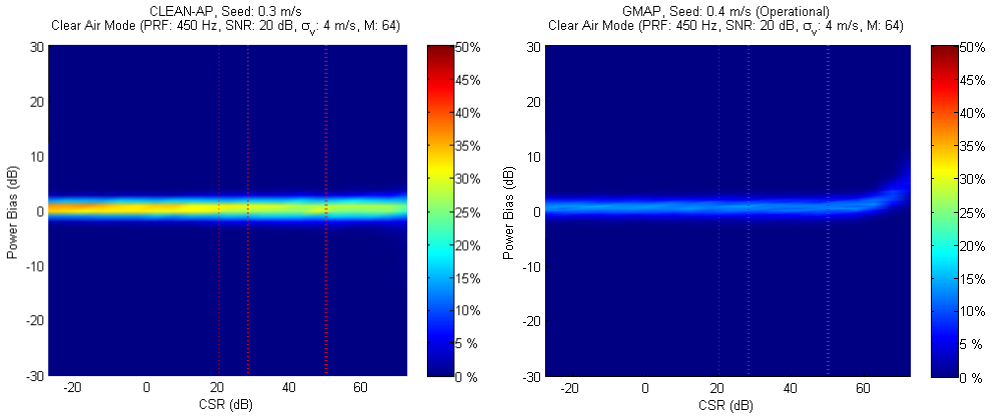

Fig. 16. CLEAN-AP (left) and GMAP (right) power bias for Clear Air Mode (PRF 450 Hz, SNR 20dB, spectrum width of 4 m/s, 64 samples).

2.4.3. *Power (Reflectivity) Bias*

To facilitate the implementation of the CLEAN-AP filter into the WSR-88D, a Gaussian model clutter suppression control was implemented for CLEAN-AP. The control parameter uses the expected spectrum width of clutter along with radar system parameters to control the CLEAN-AP filter characteristics over the full set of WSR-88D volume coverage pattern (VCP) used for different modes of operation.

Figs. 17 (Surveillance), 18 (Doppler) and 19 (Clear Air) show the reflectivity bias as a function of the true spectrum width for a 20-dB signal with a 30-dB SCR when using seed widths of 0.1 m/s to 0.5 m/s in steps of 0.1 m/s to control the CLEAN-AP filter. The WSR-88D SS requirements are listed in table 1 and are marked by circled x's in the figures. In all modes, all seed widths meet the WSR-88D SS and lead to much better performance than GMAP.

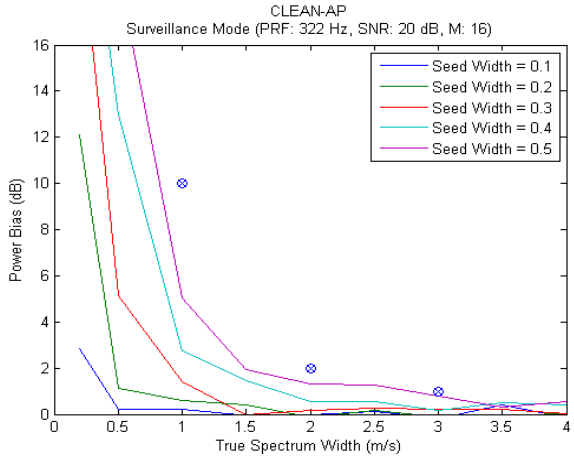

Fig. 17. CLEAN-AP power bias vs. true spectrum width for Surveillance Mode (PRF 3220 Hz, SNR 20dB, 16 samples).

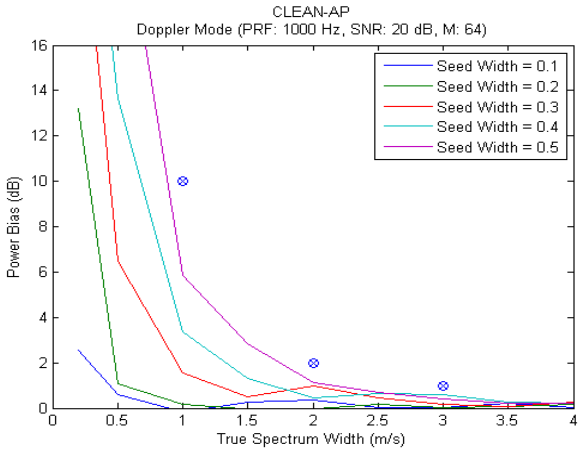

Fig. 18. CLEAN-AP power bias vs. true spectrum width for Doppler Mode (PRF 1000 Hz, SNR 20dB, 64 samples).

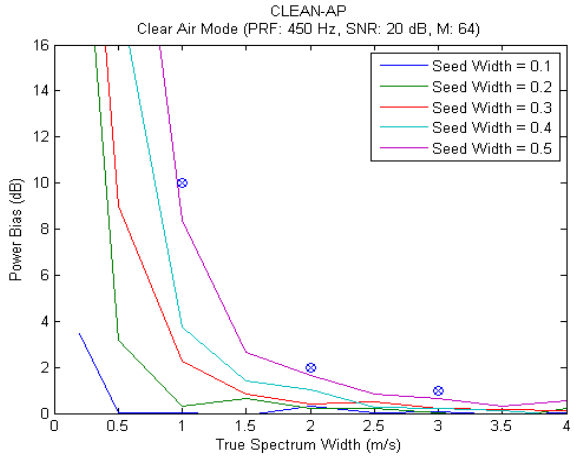

Fig. 19. CLEAN-AP power bias vs. true spectrum width for Clear Air Mode (PRF 450 Hz, SNR 20dB, 64 samples).

To see the full effect of bias performance for each filter, a 3-D surface plot of the power bias as a function of both spectrum width and velocity is shown in Figs. 20 (Surveillance), 21 (Doppler), and 22 (Clear Air). The CLEAN-AP filter (left panel) uses a seed width of 0.3 m/s and the GMAP filter (right panel) uses the operational seed width of 0.4 m/s. As seen in the figures, the GMAP filter induces higher power biases at all velocities than does the CLEAN-AP filter. These power biases are directly related to the notch-width selection process of each filter (see Fig. 8 for a comparison of the notch width selection between the CLEAN-AP filter and the GMAP filter in the Surveillance mode). At this power level (20 dB), the GMAP filter overestimates the notch width more so than the CLEAN-AP filter in all modes for all velocities at all spectrum widths where power biases are observed. The result of the notch-width overestimation is an increase in power biases (see section 2.3 for a comparative discussion between CLEAN-AP and CMD/GMAP power biases due to CMD false alarms). In all modes, the velocities affected by the CLEAN-AP filter are within 1 m/s; whereas, the GMAP filter affected velocities are within ± 2.2 m/s in Surveillance, ± 2.5 m/s in Doppler, and ± 1.5 m/s in Clear Air.

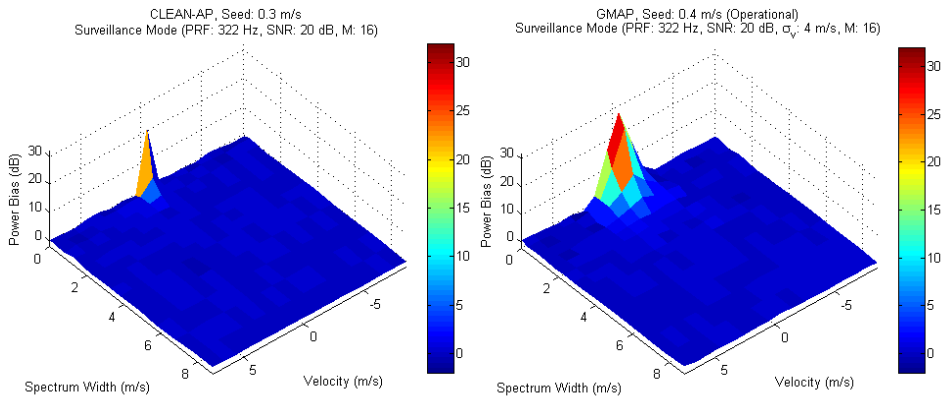

Fig. 20. CLEAN-AP (left) and GMAP (right) 3-D surface map of power bias (dB) vs. spectrum width (m/s) and velocity (m/s) for Surveillance Mode (PRF 3220 Hz, SNR 20dB, 16 samples).

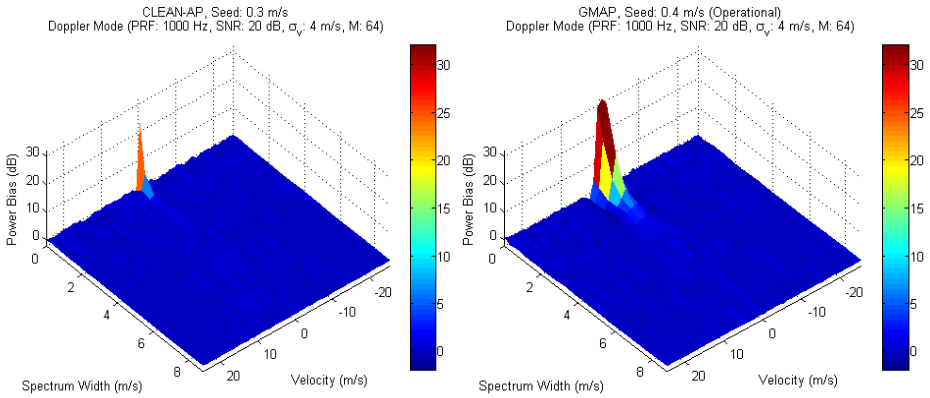

Fig. 21. CLEAN-AP (left) and GMAP (right) 3-D surface map of power bias (dB) vs. spectrum width (m/s) and velocity (m/s) for Doppler Mode (PRF 1000 Hz, SNR 20dB, 64 samples).

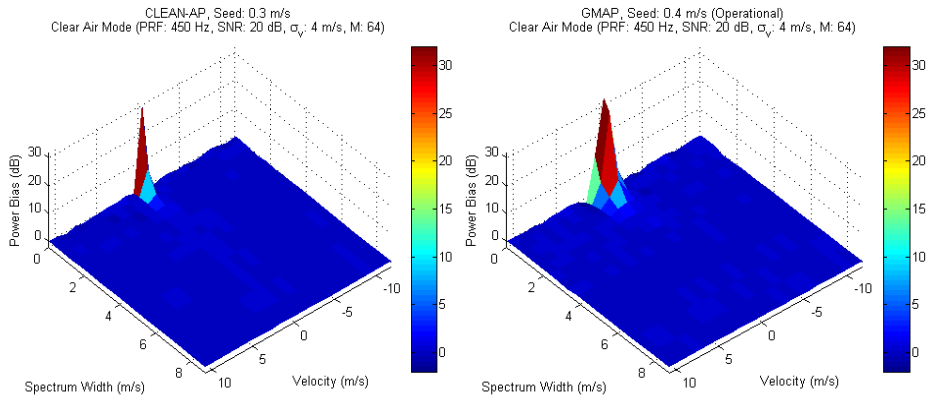

Fig. 22. CLEAN-AP (left) and GMAP (right) 3-D surface map of power bias (dB) vs. spectrum width (m/s) and velocity (m/s) for Clear Air Mode (PRF 450 Hz, SNR 20dB, 64 samples).

2.4.4. *Velocity Bias*

WSR-88D velocity bias performance criteria are listed in table 2. Both filters easily met the performance benchmarks for 20 dB and 28 dB clutter suppression levels (Ice et al. 2004a, Torres et al. 2010). In Fig. 23, the velocity bias (output of the filter) for the CLEAN-AP filter (left) and the GMAP filter (right) is plotted as a function of the true input velocity. The red dashed box in the center of the plots indicates the unusable velocity region as specified in table 2 (± 4 m/s for a 50-dB CSR). The horizontal red

dashed lines on either side of the red dashed box indicate the bias tolerance (± 2 m/s) as specified by the WSR-88D SS. The blue line indicates the velocity bias for 100 realizations and the green bars indicate the standard deviation of the velocity estimate. At the 50 dB clutter suppression level, GMAP starts to show slight biases from -10 m/s to 10 m/s as seen in Fig. 23. In general, the bias is indicative of residual ground clutter present in the output of the GMAP filter. Another indicator of residual ground clutter is the reduced variance at velocities near 0 m/s. The reader should contrast the GMAP filter velocity-bias performance with that of the CLEAN-AP filter. The CLEAN-AP filter shows no indication, in either bias or standard deviation, of ground clutter residue at 50 dB CSR. When the CSR is increased to 60 dB (Fig. 24), the GMAP filter (right) cannot suppress the ground clutter and large biases and increased variances are observed in the velocity estimates. However, the CLEAN-AP filter still provides quality unbiased velocity estimates at the 60 dB CSR level.

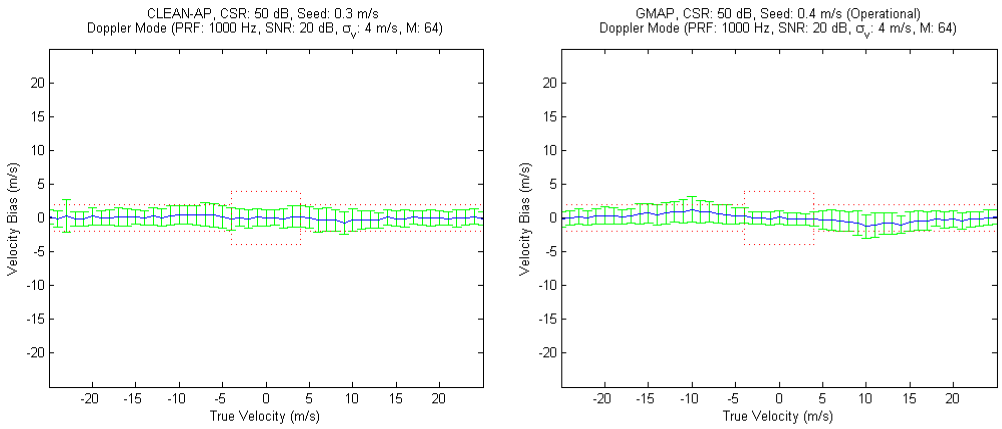

Fig. 23. CLEAN-AP (left) and GMAP (right) velocity bias (m/s) vs. true velocity (m/s) for Doppler Mode (PRF 1000 Hz, SNR 20dB, spectrum width of 4 m/s, 64 samples) with 50 dB CSR. The GMAP filter has a slight bias toward 0 m/s from -10 m/s to 10 m/s indicative of residual ground clutter present in the output of the filter. The CLEAN-AP performance shows no velocity bias for all velocity inputs.

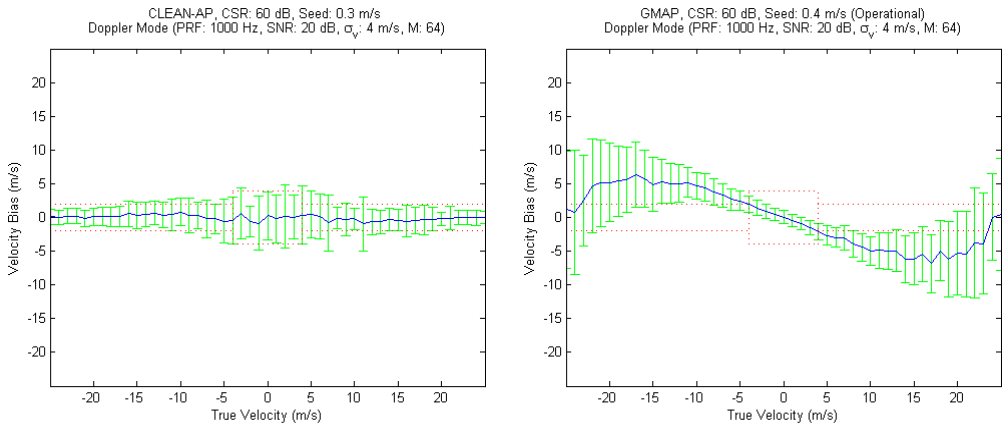

Fig. 24. CLEAN-AP (left) and GMAP (right) velocity bias (m/s) vs. true velocity (m/s) for Doppler Mode (PRF 1000 Hz, SNR 20dB, spectrum width of 4 m/s, 64 samples) with 60 dB CSR. The GMAP filter is unusable as indicated by the velocity bias at all velocities inputs. The CLEAN-AP performance shows no velocity bias with only a slight increase in variance in the unusable velocity region.

2.4.5. *Spectrum Width Bias*

When clutter filtering is applied, the WSR-88D SS requirements for spectrum-width bias and standard deviation are 2 m/s for an input spectrum width of 4 m/s. An additional 1 m/s allowance is provided for spectrum width biases when a clutter residue of -15 dB CSR is present in the output of the filter. The estimator used for these tests is the R0/R1 estimator described in Doviak and Zrnić (1993). At times, this estimator can give a spectrum width estimate that is nonsensical. These values are normally set to 0 m/s in the estimation routine for the WSR-88D system. For the bias and standard deviation estimates, these artificial zeros are removed.

Figs. 25 and 26 show a top view of 3-D histograms of spectrum width bias (dB) for CLEAN-AP (left) and GMAP (right) as a function of true spectrum width (0.2, 0.5, 1, 1.5, 2, 2.5, 3, 3.5, 4 , 5, 6, 7, 8, and 9 m/s). The percentage of 5100 realizations of each spectrum width bias shown in color (dark blue = 0% to red = 50%). Overlaid on the

histograms is the mean spectrum width bias (red circles) and standard deviation (red bars). A bias line (green) at 0 m/s is shown as well as the upper and lower bias limits at ±2 m/s (red). In Fig. 25, the spectrum-width bias and standard deviation from both filters are displayed for a 50-dB CSR. Both filters meet the WSR-88D SS requirements of 2 m/s for both bias and standard deviation at the benchmark of 4 m/s; however, the output of the CLEAN-AP filter is less biased and more precise for all spectrum widths. At a 55-dB CSR, shown in Fig. 26, spectrum widths become unusable when using the GMAP filter; whereas, the spectrum widths of the CLEAN-AP filter still exceed WSR-88D SS requirements. Although not shown here, the CLEAN-AP filter still meets the WSR-88D SS requirement at the benchmark of 4 m/s for a CSR of 60 dB (Torres et. al 2010). In fact, at a 60-dB CSR, the bias is less than 2 m/s for all spectrum widths tested with the standard deviation below 2 m/s for input spectrum widths ranging from 3 m/s to ~9 m/s.

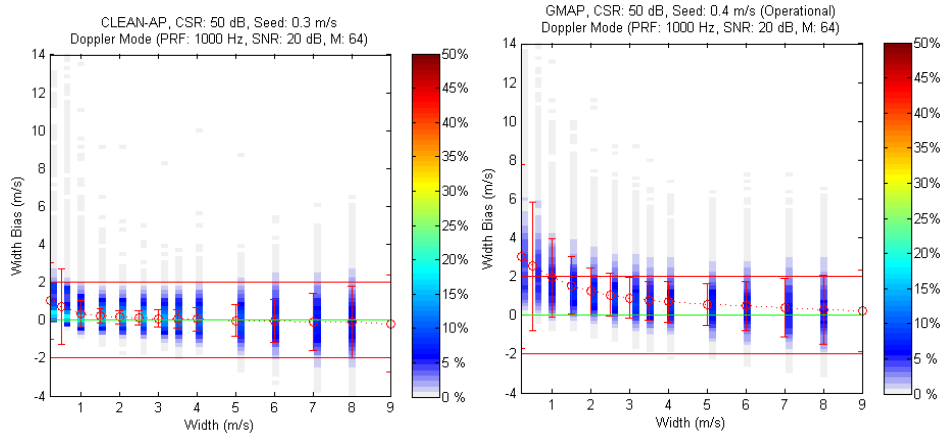

Fig. 25. CLEAN-AP (left) and GMAP (right) spectrum width bias (m/s) vs. true spectrum width (m/s) for Doppler Mode (PRF 1000 Hz, SNR 20dB, 64 samples) with 50 dB CSR. The GMAP filter meets WSR-88D requirements at a benchmark spectrum width of 4 m/s, but indicates a positive bias for all spectrum width inputs. The CLEAN-AP performance meets WSR-88D requirements with reduced variance and no spectrum width bias for all input spectrum widths except those less than ~1 m/s.

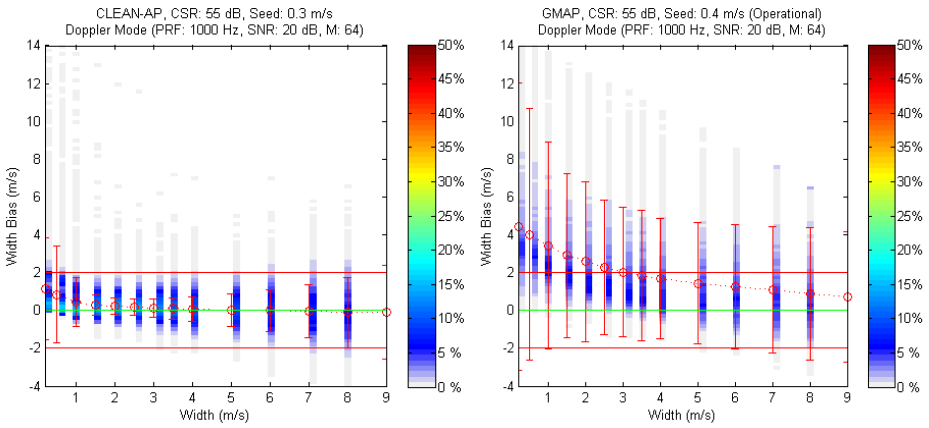

Fig. 26. CLEAN-AP (left) and GMAP (right) spectrum width bias (m/s) vs. true spectrum width (m/s) for Doppler Mode (PRF 1000 Hz, SNR 20dB, 64 samples) with 55 dB CSR. The GMAP filter just meets WSR-88D bias requirement at a benchmark spectrum width of 4 m/s, but does not meet the standard deviation requirement. The CLEAN-AP performance meets WSR-88D requirements with reduced variance and no spectrum width bias for all input spectrum widths except those less than ~1 m/s.

2.4.6. *Real-Data Example of CLEAN-AP Performance*

The CLEAN-AP filter provides a real-time, automatic, integrated approach to ground clutter detection and filtering to produce improved quality estimates over the full dynamic range of the WSR-88D receiver (at least 93 dB, WSR-88D SS 2008). The effective clutter-suppression capability of the CLEAN-AP filter is in part provided by the active choice of the lowest dynamic-range data window that maintains the ground clutter spectral leakage to levels sufficient to remove the contamination while preserving the weather signal. The choice of the data window is provided by first estimating the amount of clutter contamination in the signal (Warde and Torres 2009). The effectiveness of this process was reported in the NSSL report 14 (Torres et al. 2010). An example of mountainous terrain ground clutter contamination from Tucson, AZ will illustrate the data-window selection process.

In Fig. 27, non-filtered (left) and CLEAN-AP filtered (right) reflectivity images are shown for Tucson, AZ. The mountainous terrain surrounding the WSR-88D radar is visible as yellow to red in the non-filtered reflectivity image. In the filtered image, the CLEAN-AP filter identified and removed the clutter contamination. In Fig. 28, the power removed during the CLEAN-AP filtering process reveals that the clutter contamination in the mountainous regions typically exceeds 50 dB CNR levels. For this level of ground clutter contamination, a Blackman data window will cause excessive spectral leakage and will make ground clutter removal difficult while obscuring weather signals. For these strong-clutter regions, the Blackman-Nuttal data window provides better spectral containment of ground clutter resulting in better ground clutter suppression.

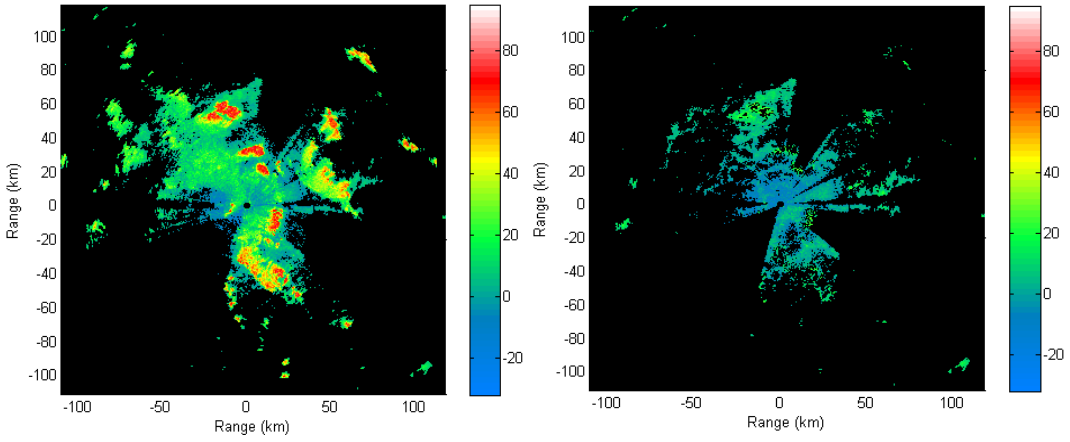

Fig. 27. Non-filtered (left) and CLEAN-AP filtered (right) reflectivity from Tucson, AZ.

In Fig. 29, the data window selection process of the CLEAN-AP filter is observed. Although the selection process is provided at all range gates, only the range gates where reflectivity is above threshold is shown in the CLEAN-AP filtered image (Fig. 27 right). In the regions of strongest clutter contamination (i.e., mountainous terrain) where the CNR reaches levels over 50 dB, the CLEAN-AP filter properly selects the Blackman-

Nuttal data window with a highest sidelobe level of -98 dB below the main lobe level; whereas, in regions of weakest clutter contamination (including regions devoid of clutter contamination), the CLEAN-AP filter selects the rectangular window with a highest sidelobe level of -13 dB (best window for the lowest variance of estimates).

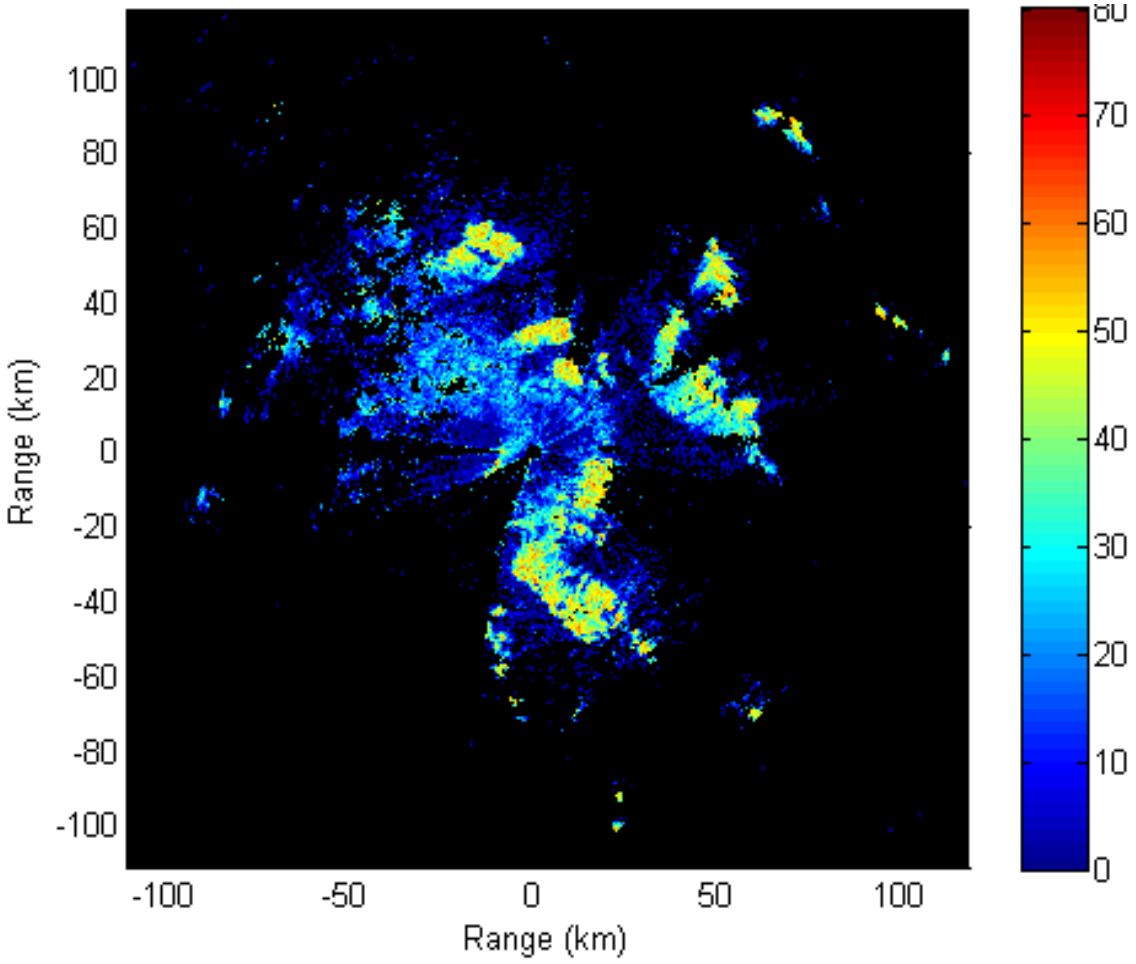

Fig. 28. Power removed by CLEAN-AP (Tucson, AZ).

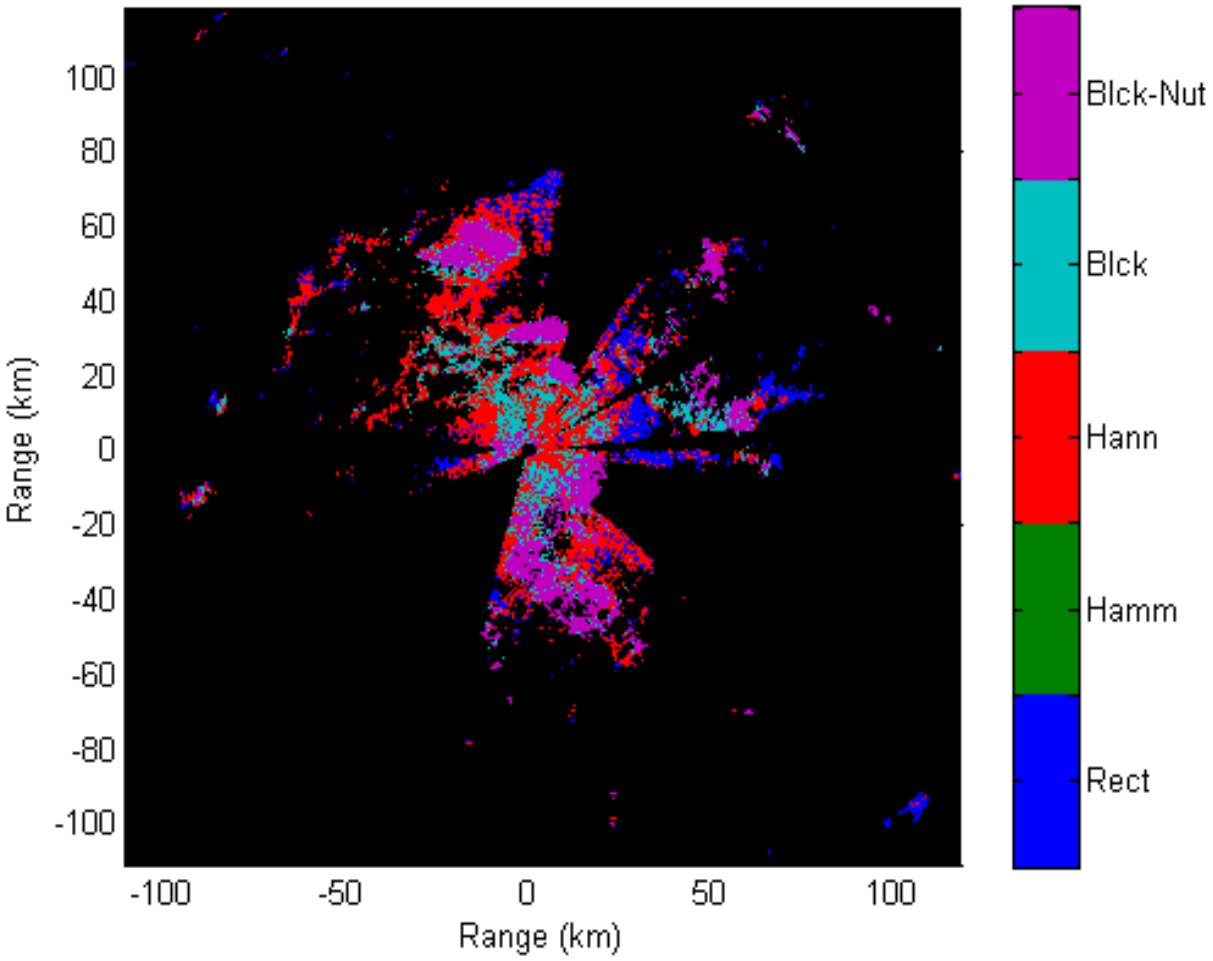

Fig. 29. CLEAN-AP data window selection (Tucson, AZ).

Because of the dynamic data-window-selection process the notch width used to filter the ground clutter can be maintained at the smallest possible values during the clutter filtering process. Shown in Fig. 30 is the normalized notch width (notch width/$2v_a$) used in CLEAN-AP to filter the reflectivity in Fig. 27. In this case, the Nyquist velocity (v_a) is about 8.2 m/s. Note that the notch width is maintained at a low value throughout the image even though the ground clutter contamination varies from weak to strong. Recall from table 2 that the WSR-88D SS requires velocities above 2 m/s to be usable for the lowest clutter-suppression level of 20 dB, and progresses to velocities above 4 m/s for the

highest clutter-suppression level of 50 dB. In Fig. 31, the normalized notch widths are quantized to the usable velocity levels for 1, 2, 3, 4 and >4 m/s, where the value indicates the lowest usable velocity in the interval (i.e. 1 – Va, 2 – Va, etc.). Here, CLEAN-AP shows that usable velocities above 2 m/s are maintained even at the levels well above a 50-dB CNR.

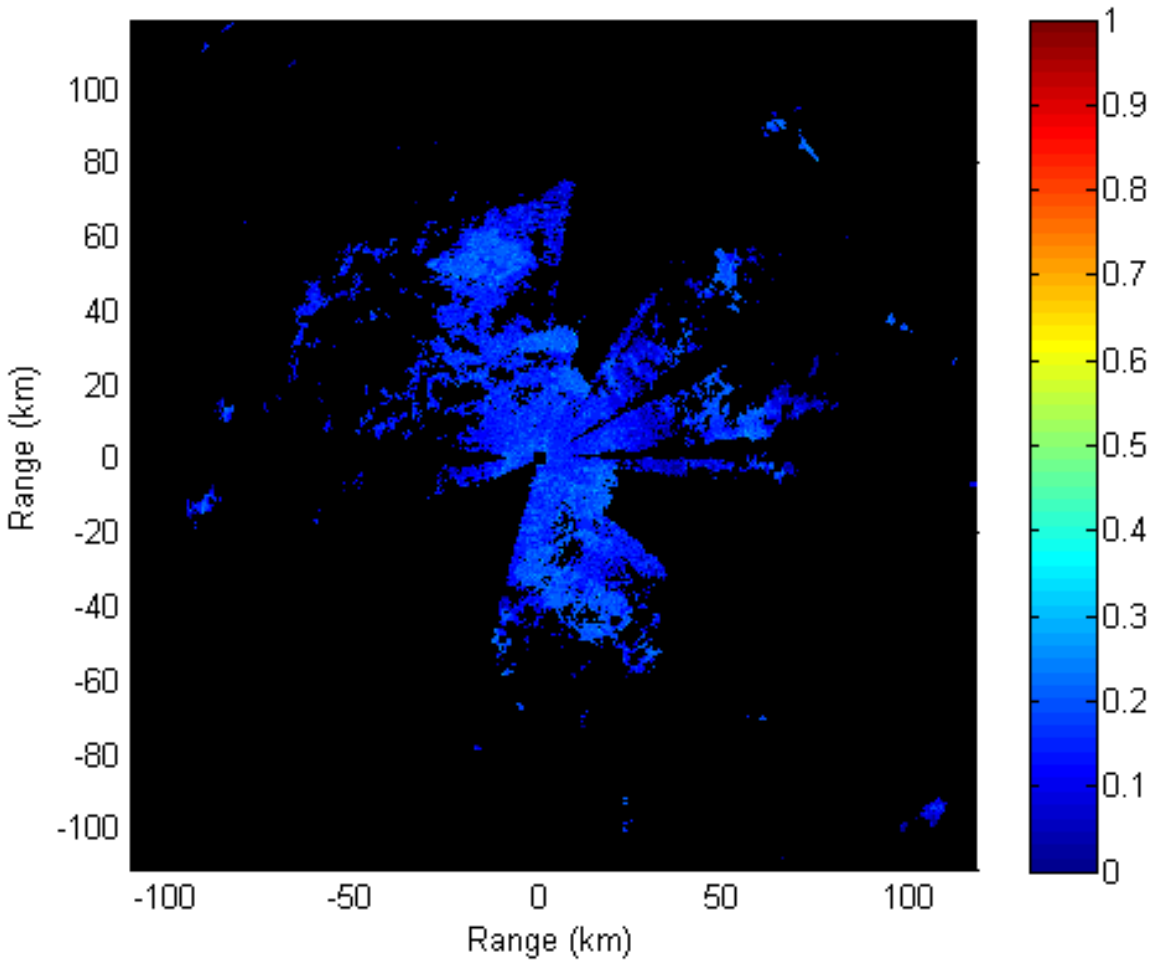

Fig. 30. Normalized notch widths (notch width/$2v_a$) for CLEAN-AP (Tucson, AZ).

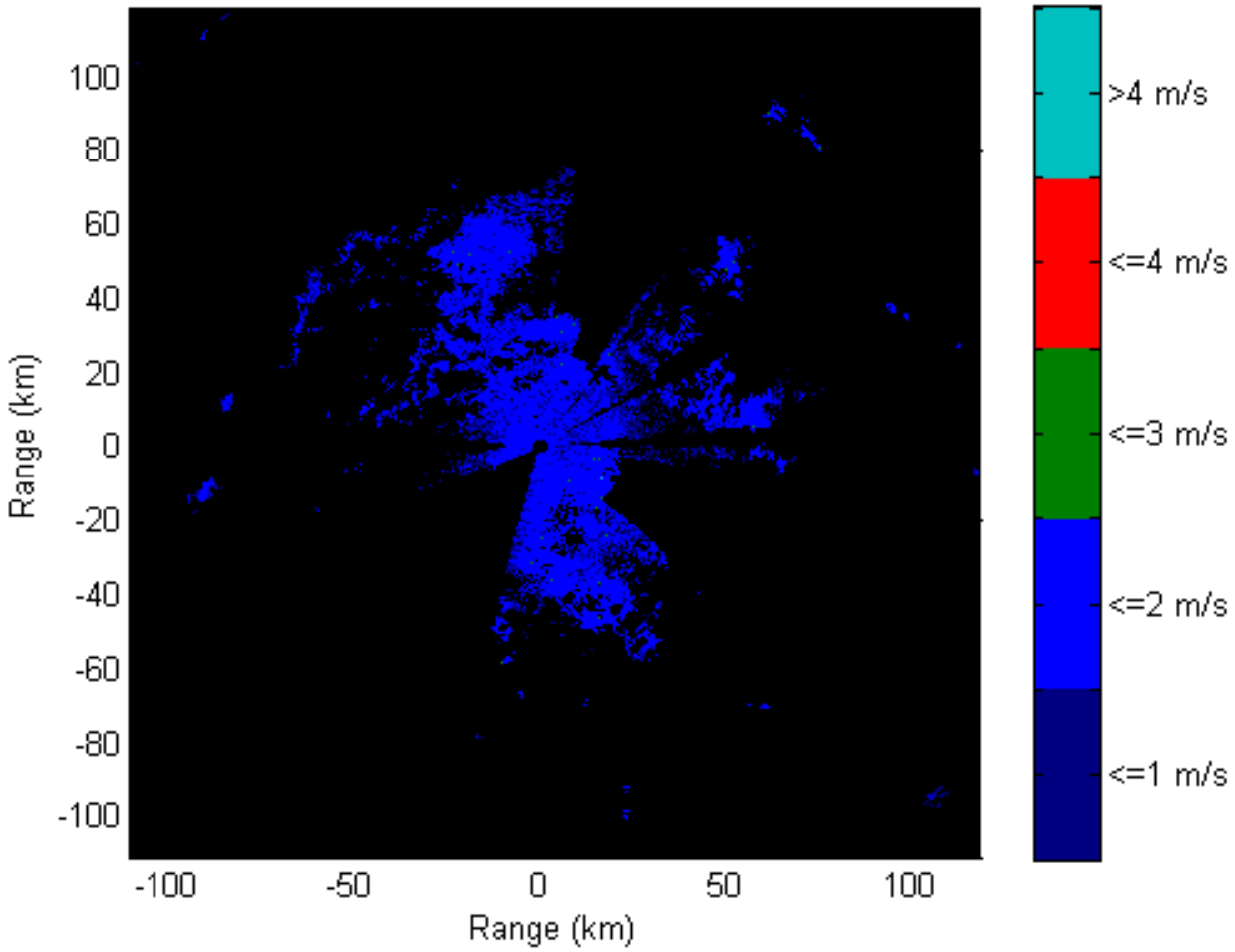

Fig. 31. Usable velocity levels from CLEAN-AP (Tucson, AZ).

To compare ground clutter mitigation performance of the CLEAN-AP filter with that of CMD/GMAP for this case, the ROC provided level II with CMD/GMAP enabled. In Fig. 32, the CLEAN-AP (left) and CMD/GMAP (right) filtered reflectivity from Tucson, AZ are shown. Both ground clutter mitigation approaches performed remarkably well with very similar results; however, two regions of ground clutter contamination highlight performance differences: mountainous terrain and weak ground clutter. The red arrows in the images of Fig. 32 point to a mountainous terrain region where 'hot spots' had been of operational concern during beta testing of the CMD algorithm. After modification of the CMD algorithm, ground clutter detection was realized, but the GMAP filter does not

adequately suppress the ground clutter. Contrast the CMD/GMAP performance with that of the CLEAN-AP filter which effectively provided both detection and filtering in the mountainous terrain region. Now focus on the region pointed to by the yellow arrows in Fig. 32. The yellow arrows point to a region of weak ground clutter that was detected and filtered by the CLEAN-AP filter; however, the CMD algorithm did not detect the contamination thus the GMAP filter was not applied leaving the region non-filtered.

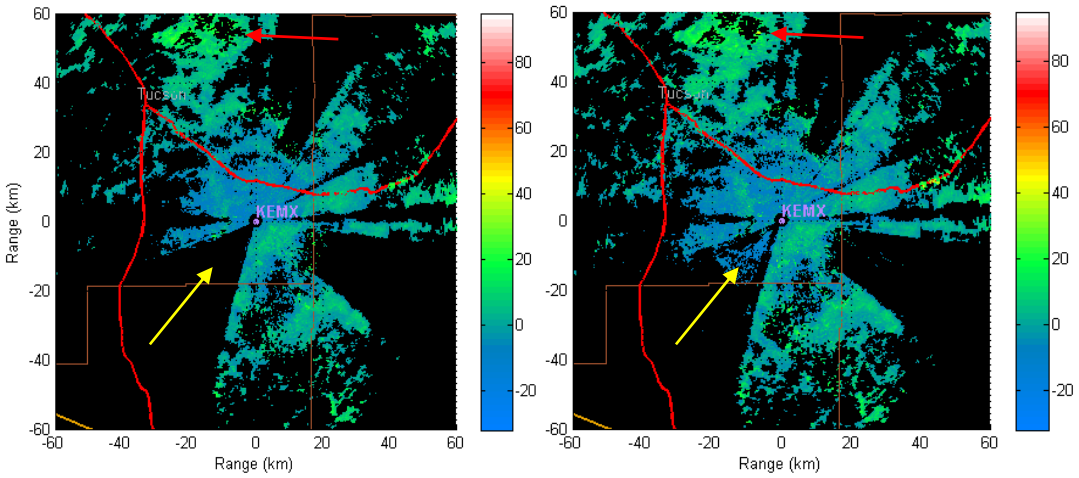

Fig. 32. CLEAN-AP (left) and CMD/GMAP (right) filtered reflectivity from Tucson, AZ. The red arrows point to a region of mountainous terrain the was suppressed using the CLEAN-AP filter that was under-suppressed by the GMAP filter. The yellow arrows point to weak ground clutter that was detected and filtered by the CLEAN-AP filter that was undetected by the CMD algorithm and left non-filtered.

As another example of the ground clutter mitigation performance comparison between the two ground clutter mitigation approaches, the ROC provided level II data with CMD/GMAP enabled for the WSR-88D testbed (KCRI) in Norman, OK. The non-filtered reflectivity (top) and CLEAN-AP (bottom-left) and CMD/GMAP (bottom-right) filtered reflectivity are shown in Fig. 33. A region of reduced reflectivity near the radar (center of the image) and extending north and south of the radar appears as a result of

filtering, but appears to be exaggerated by the CMD/GMAP process more so than by CLEAN-AP. A region to the south of the radar where reduced reflectivity appears to be in a area of good weather returns prompts further investigation into the detection aspects of the of both approaches.

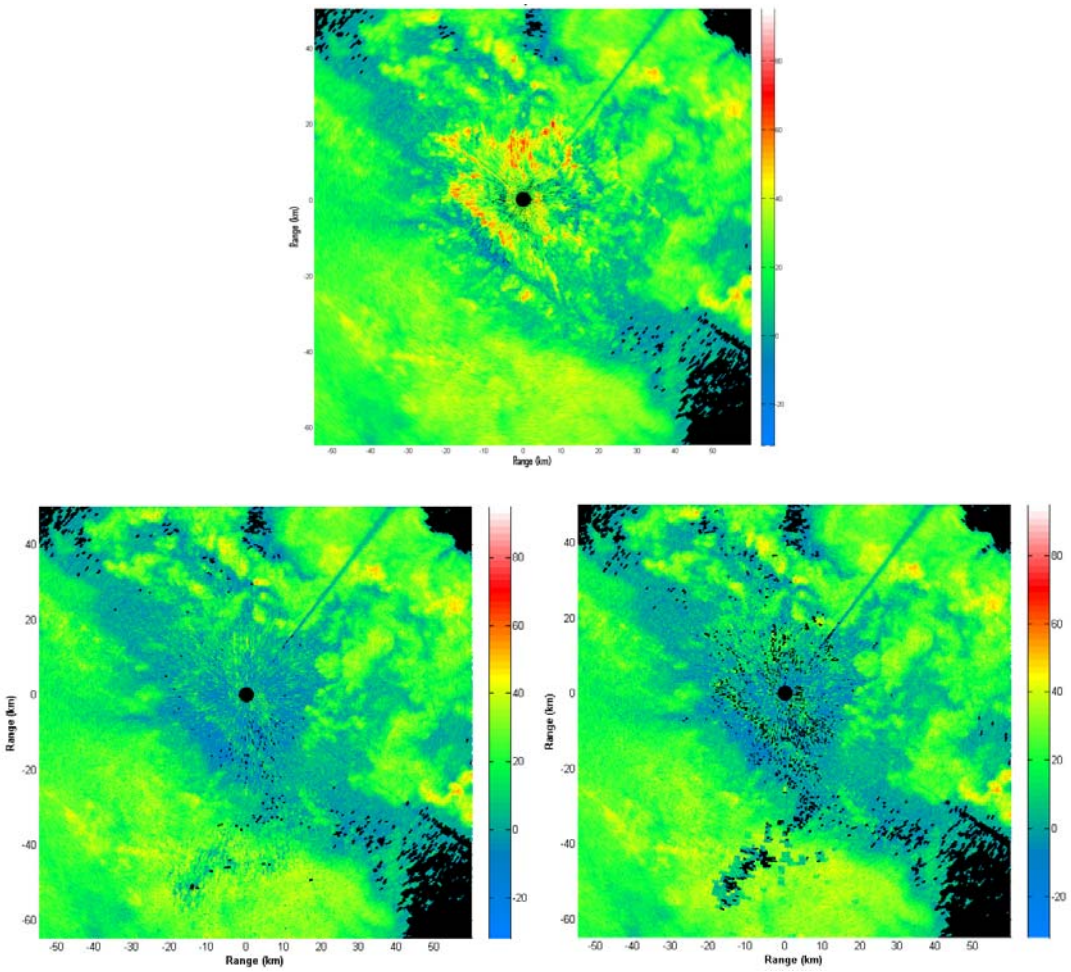

Fig. 33. Non-filtered reflectivity (top) and CLEAN-AP (bottom-left) and CMD/GMAP (bottom-right) filtered reflectivity from ROC testbed in Norman, OK.

The non-filtered velocities (top), and CLEAN-AP (bottom-left) and CMD/GMAP (bottom-right) filtered velocities are shown in Fig. 34. It is difficult to see the extent of ground clutter contamination in reflectivity (Fig. 33), but close examination of the non-filtered velocities (Fig. 34 top view) indicates that low-level ground-clutter contamination

was present south of the radar in the region in question. Here, CLEAN-AP automatically adjusts the suppression level to deal with low-level clutter contamination; whereas CMD/GMAP heavily suppresses the low-level ground clutter. Another artifact, readily apparent in the south-southeast portion of the images, is the spatial discontinuities from the CMD/GMAP "on/off" approach compared to the integrated ground-clutter mitigation approach used by CLEAN-AP. Spatial discontinuities like these, produced by CMD/GMAP, continue to afflict the base data in the operational WSR-88D network.

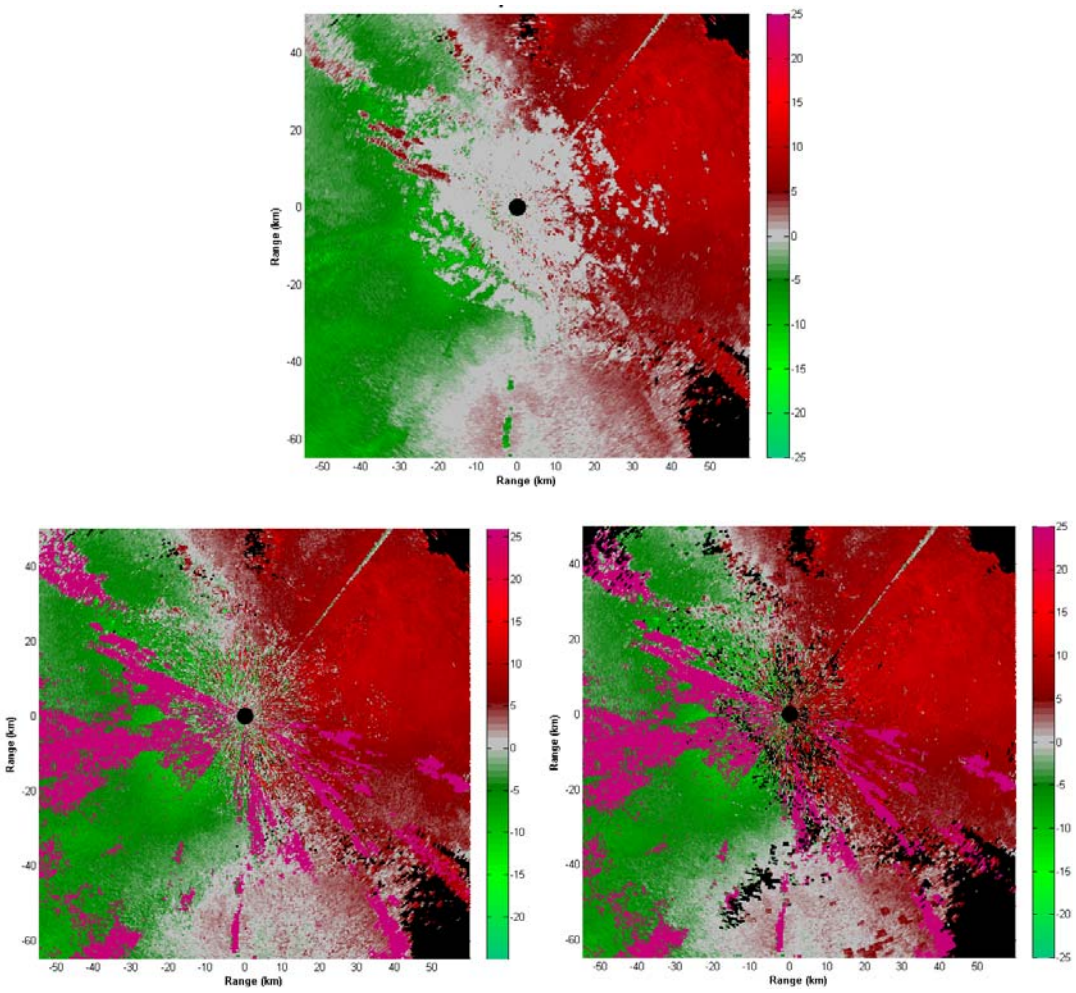

Fig. 34. Non-filtered velocity (top) and CLEAN-AP (left) and CMD/GMAP (right) filtered velocity from ROC testbed in Norman, OK.

An example of CLEAN-AP performance along the zero-isodop is emphasized with a snow case from the operational WSR-88D radar (KTLX) Twin Lakes, OK. No CMD/GMAP level II data was provided for performance comparisons. The non-filtered (left) and CLEAN-AP filtered (right) reflectivity (velocity) in Fig. 35 (Fig. 36) reveals that the automated ground clutter mitigation process of CLEAN-AP produced no areas of reduced reflectivity, especially along the zero-isodop, while completely removing the ground-clutter contamination.

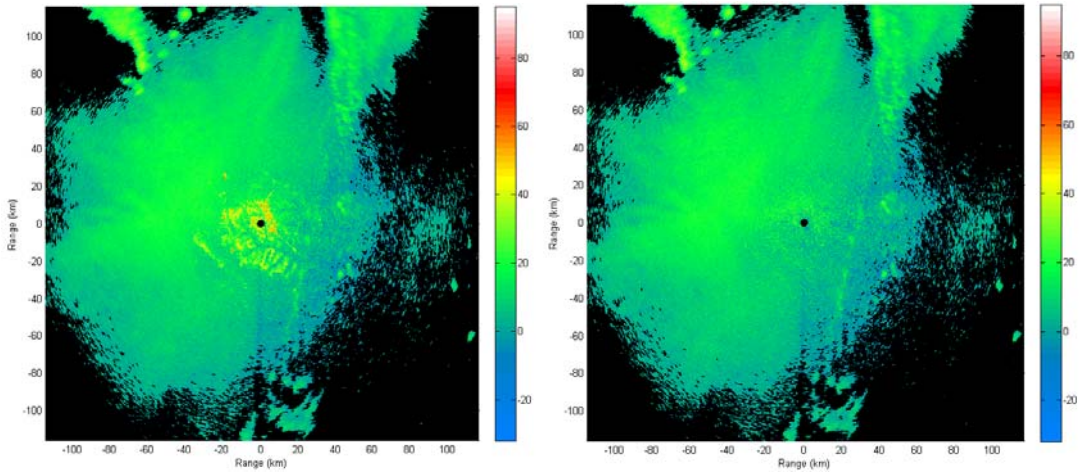

Fig. 35. Non-filtered (left) and CLEAN-AP filtered (right) reflectivity from KTLX, Twin Lakes, OK

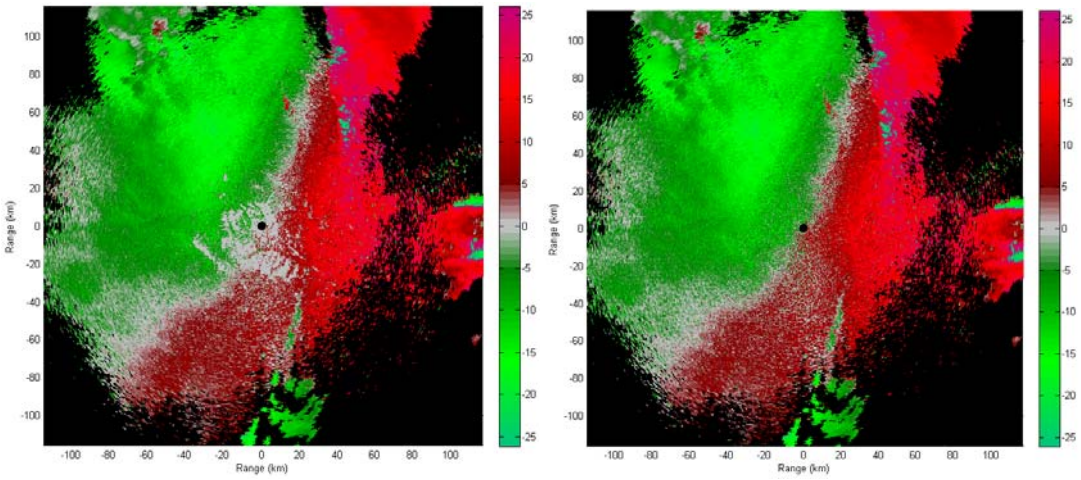

Fig. 36. Non-filtered (left) and CLEAN-AP filtered (right) velocity from KTLX, Twin Lakes, OK

2.5. CLEAN-AP Performance Summary

Using the WSR-88D SS as guidance, the CLEAN-AP filter is shown to exceed the ground-clutter suppression requirements needed to support NEXRAD operations. Ground clutter suppression at ~60-dB CSR is provided in both the reflectivity channel (requirement of 30 dB) and in the Doppler channel (requirement of 50 dB). At all levels of clutter suppression below the 60-dB CSR level, CLEAN-AP provides unbiased estimates with low variance in all weather modes used by the WSR-88D: Surveillance, Doppler and Clear Air. Performance comparisons between CLEAN-AP and GMAP reveal that CLEAN-AP has higher ground-clutter suppression capabilities with lower variance. Although there are no ground-clutter-detection requirements in the WSR-88D SS, the real-data analysis indicates that better ground-clutter mitigation (detection and filtering) is achieved when using CLEAN-AP over the current CMD/GMAP approach. The on/off filtering approach of the CMD/GMAP creates artifacts in the base data. These artifacts are mitigated by CLEAN-AP due to the integration of dynamic ground-clutter detection and filtering. Additionally, losses along the zero-isodop are greatly reduced. The adaptive windowing used in CLEAN-AP provides smaller variance of estimates at low CSR levels and higher clutter suppression at high CSR levels while still meeting WSR-88D requirements.

3. References

Barron Services report, 2011: Zdr Calibration Accuracy Analysis, BS-2000-000-107.

Doviak, D. and D. Zrinć, 1993: Doppler Radar and Weather Observations, 2nd edition. Academic Press.

Harris, F., 1978: On the use of windows for harmonic analysis with the discrete Fourier transform, Proc. IEEE, vol. 66, 51-83.

Hubbert, J., M. Dixon, and S. Ellis, 2009: Weather radar ground clutter. Part II: Real-Time Identification and Filtering, Journal of Atmos. Oceanic Technol., vol. 26, 1118-1196.

Ice, R., D. Warde, D. Sirmans, D. Rachel, 2004a: Report on Open RDA – RVP8 Signal Processing, Part 1 – Simulation Study, WS-88D Radar Operations Center Report, January 2004. 87 pp.

___, D. Warde, D. Sirmans, D. Rachel, 2004b: Report on Open RDA – RVP8 Signal Processing, Part 2 – Engineering Analysis with Meteorological Data, WS-88D Radar Operations Center Report, July 2004. 56 pp.

Siggia, A., and J. Passarelli, 2004: Gaussian model adaptive processing (GMAP) for improved ground clutter cancellation and moment calculation. Proc. Third European Conf. on Radar in Meteorology and Hydrology, Visby,Gotland, Sweden, ERAD, 67–73.

Sirmans, D., 1992: Clutter filtering in the WSR-88D, OSF Internal Report. 125 pp.

Snow, J. and R. Scott, 2003: Strategic Directions for WSR-88D Doppler Weather Surveillance Radar in the Period 2007–2025, Preprints, 31st International Conference on Radar Meteorology, Seattle, WA, USA, Amer. Meteor. Soc.

Warde, D. A. and D. M. Torres, 2009: Automatic detection and removal of ground clutter contamination on weather radars. Preprints, 34th Conference on Radar Meteorology, Williamsburg, VA, USA, Amer. Meteor. Soc.

Warde, D. A. and D. M. Torres, 2010: A novel ground-clutter-contamination mitigation solution for the NEXRAD network: the CLEAN-AP filter. Preprints, 26th Conference on IIPS for Meteorology, Oceanography, and Hydrology, Atlanta, GA, USA, Amer. Meteor. Soc.

WSR-88D System Specifications 2810000H, 25 April 2008, Radar Operations Center, 160 pp.

LIST OF NSSL REPORTS FOCUSED ON POSSIBLE UPGRADES

TO THE WSR-88D RADARS

Torres S., D. Warde, B. Gallardo, K. Le, and D. Zrnić, 2010: Signal Design and Processing Techniques for WSR-88D Ambiguity Resolution: Staggered PRT Algorithm Updates, the CLEAN-AP Filter, and the Hybrid Spectrum Width Estimator. NOAA/NSSL Report, Part 14, 145 pp.

Torres S., D. Warde, and D. Zrnić, 2010: Signal Design and Processing Techniques for WSR-88D Ambiguity Resolution: Staggered PRT Updates. NOAA/NSSL Report, Part 13, 142 pp.

Torres S., D. Warde, and D. Zrnić, 2009: Signal Design and Processing Techniques for WSR-88D Ambiguity Resolution: Staggered PRT Updates and Generalized Phase Codes. NOAA/NSSL Report, Part 12, 156 pp.

Torres S. and D. Zrnić, 2007: Signal Design and Processing Techniques for WSR-88D Ambiguity Resolution: Evolution of the SZ-2 Algorithm. NOAA/NSSL Report, Part 11, 145 pp.

Zrnić, D.S., Melnikov, V. M., J. K. Carter, and I. Ivić, 2007: Calibrating differential reflectivity on the WSR-88D, (Part 2). NOAA/NSSL Report, 34 pp.

Torres S. and D. Zrnić, 2006: Signal Design and Processing Techniques for WSR-88D Ambiguity Resolution: Evolution of the SZ-2 Algorithm. NOAA/NSSL Report, Part 10, 71 pp.

Torres S., M. Sachidananda, and D. Zrnić, 2005: Signal Design and Processing Techniques for WSR-88D Ambiguity Resolution: Phase coding and staggered PRT. NOAA/NSSL Report, Part 9, 112 pp.

Zrnić, D., V. Melnikov, and J. Carter, 2005: Calibrating differential reflectivity on the WSR-88D. NOAA/NSSL Report, 34 pp.

Torres S., M. Sachidananda, and D. Zrnić, 2004: Signal Design and Processing Techniques for WSR-88D Ambiguity Resolution: Phase coding and staggered PRT: Data collection, implementation, and clutter filtering. NOAA/NSSL Report, Part 8, 113 pp.

Zrnić, D., S. Torres, J. Hubbert, M. Dixon, G. Meymaris, and S. Ellis, 2004: NEXRAD range-velocity ambiguity mitigation. SZ-2 algorithm recommendations. NCAR-NSSL Interim Report.

Melnikov, V, and D. Zrnić, 2004: Simultaneous transmission mode for the polarimetric WSR-88D – statistical biases and standard deviations of polarimetric variables. NOAA/NSSL Report, 84 pp.

Bachman, S., 2004: Analysis of Doppler spectra obtained with WSR-88D radar from non-stormy environment. NOAA/NSSL Report, 86 pp.

Zrnić, D., S. Torres, Y. Dubel, J. Keeler, J. Hubbert, M. Dixon, G. Meymaris, and S. Ellis, 2003: NEXRAD range-velocity ambiguity mitigation. SZ(8/64) phase coding algorithm recommendations. NCAR-NSSL Interim Report.

Torres S., D. Zrnić, and Y. Dubel, 2003: Signal Design and Processing Techniques for WSR-88D Ambiguity Resolution: Phase coding and staggered PRT: Implementation, data collection, and processing. NOAA/NSSL Report, Part 7, 128 pp.

Schuur, T., P. Heinselman, and K. Scharfenberg, 2003: Overview of the Joint Polarization Experiment (JPOLE), NOAA/NSSL Report, 38 pp.

Ryzhkov, A, 2003: Rainfall Measurements with the Polarimetric WSR-88D Radar, NOAA/NSSL Report, 99 pp.

Schuur, T., A. Ryzhkov, and P. Heinselman, 2003: Observations and Classification of echoes with the Polarimetric WSR-88D radar, NOAA/NSSL Report, 45 pp.

Melnikov, V., D. Zrnić, R. Doviak, and J. Carter, 2003: Calibration and Performance Analysis of NSSL's Polarimetric WSR-88D, NOAA/NSSL Report, 77 pp.

NCAR-NSSL Interim Report, 2003: NEXRAD Range-Velocity Ambiguity Mitigation SZ(8/64) Phase Coding Algorithm Recommendations.

Sachidananda, M., 2002: Signal Design and Processing Techniques for WSR-88D Ambiguity Resolution, NOAA/NSSL Report, Part 6, 57 pp.

Doviak, R., J. Carter, V. Melnikov, and D. Zrnić, 2002: Modifications to the Research WSR-88D to obtain Polarimetric Data, NOAA/NSSL Report, 49 pp.

Fang, M., and R. Doviak, 2001: Spectrum width statistics of various weather phenomena, NOAA/NSSL Report, 62 pp.

Sachidananda, M., 2001**:** Signal Design and Processing Techniques for WSR-88D Ambiguity Resolution, NOAA/NSSL Report, Part 5, 75 pp.

Sachidananda, M., 2000**:** Signal Design and Processing Techniques for WSR-88D Ambiguity Resolution, NOAA/NSSL Report, Part 4, 99 pp.

Sachidananda, M., 1999**:** Signal Design and Processing Techniques for WSR-88D Ambiguity Resolution, NOAA/NSSL Report, Part 3, 81 pp.

Sachidananda, M., 1998**:** Signal Design and Processing Techniques for WSR-88D Ambiguity Resolution, NOAA/NSSL Report, Part 2, 105 pp.

Torres, S., 1998: Ground Clutter Canceling with a Regression Filter, NOAA/NSSL Report, 37 pp.

Doviak, R. and D. Zrnić, 1998**:** WSR-88D Radar for Research and Enhancement of Operations: Polarimetric Upgrades to Improve Rainfall Measurements, NOAA/NSSL Report, 110 pp.

Sachidananda, M., 1997**:** Signal Design and Processing Techniques for WSR-88D Ambiguity Resolution, NOAA/NSSL Report, Part 1, 100 pp.

Sirmans, D., D. Zrnić, and M. Sachidananda, 1986**:** Doppler radar dual polarization considerations for NEXRAD, NOAA/NSSL Report, Part I, 109 pp.

Sirmans, D., D. Zrnić, and N. Balakrishnan, 1986**:** Doppler radar dual polarization considerations for NEXRAD, NOAA/NSSL Report, Part II, 70 pp.

Appendix A. Z_{DR} Calibration

Herein we offer comments on the report by Baron Services (2011) concerning accuracy of Z_{DR} calibration. We contrast it to the NSSL's suggested procedure and discuss ways to make it more robust.

A.1. Comments on Baron's Zdr Calibration – Accuracy analysis report

Without knowing the detailed – step by step explanation (containing high level block diagrams) of the calibration procedure we offer general comments and fewer specifics than would be possible otherwise. The procedure looks more complicated than needed, yet the error budget analysis indicates that the precision is satisfactory. The numbers are reasonable and we believe correctly estimated. The random error budget is realistic and the precision in the worst case scenario (all errors adding coherently) is better than 0.1 dB. The cumulative standard deviation is a respectable 0.026 dB. From the plots of Z_{DR} offset (Figure 2 in the report) it is clear that the system is stable and the changes are slow compared to the update times (i.e., time of volume scans). This is confirmed by the histograms (Figures 3, 4 and 5) which indicate that less than 1% of changes in the Z_{DR} offset between VCPs are larger than 0.015 dB. Moreover, the fact that the daily periodicity follows the temperature change indicates that the procedure compensates the variation in gain of the amplifiers as it is supposed to do.

Overall the precision and stability meet the expectation and requirements. The remaining issue which is mentioned by the contractor and of which we are all aware is the accuracy of the measurement i.e., the determination of the residual absolute bias. Because the

system is stable we submit that in due time and with some effort this will be resolved. Some thoughts on the subject by follow.

A.2. The bias requirement

The value of ±0.1 dB came from two considerations:

A) One is the fractional error in rain rate estimates R(Z, Z_{DR}) which at Z_{DR} ≤1 dB can be larger than 13% if the bias is ≥0.1 dB (Zrnic et al. 2010). The error rises to 20% if the bias is ≥ 0.15 dB. But, this occurs at values of Z < 36 dBZ, or rain rates of < 6 mm/h. At higher rain rates the requirement is relaxed to Bias ≤ 0.1Z_{DR} (where Z_{DR} is in dB).

There is, however, a rain rate relation for moderate rains that depends solely on total differential phase and reflectivity, but in such way that it is independent on receiver calibration. It uses in a roundabout manner attenuation of signals. And this relation is almost linearly proportional to rain rate thus practically independent of DSD variations. Inclusion of this relation into the synthetic algorithm and application to existing data needs to be made to determine its quality. If the results turn out as theory predicts the Z_{DR}'s role would diminish from quantitative to mainly classification and the requirement on accuracy would be considerably relaxed.

B) The other consideration is separation of hydrometeor classes. Specifically Z_{DR} of dryer cool snow is about 0.2 dB higher than from warmer snow (Ryzhkov and Zrnic 1998). This and similar distinctions are build into the weighting functions of the Hydrometeor Classification Algorithm (HCA). By slightly widening these functions the HCA can be adjusted to perform well.

A.3. The calibration procedure and error budget as inferred from the report

The contractor has the following equation for the budget of Zdr error.

$$Zdr_{Bias}(dB) = 2Zdr^{Sun}(dB) - 2Zdr_{Rx}^{Sun}(dB) + Zdr^{BITE}(dB) + Zdr_{Rx}^{Test}(dB) + Zdr_{Tx}(dB) - Zdr_{Tx}^{Cal\_Bias}(dB)$$

where:

Zdr_{Bias} ***System Zdr Bias –*** Total sum of all biases in the system associated with Zdr.

Zdr^{Sun} ***Sun Check Sun Bias Measurement*** - The difference between the horizontal and vertical receiver channels when pointing the antenna at the sun.

Zdr_{Rx}^{Sun} ***Sun Check Receiver Bias –***Bias in the receiver at the time of the sun bias measurement. This one can be bypassed – accounted in Zdr_{Rx}^{RVP}

Zdr^{BITE} ***Test Signal Bias –*** Bias in the test signals measured at the receiver front end. This one is not needed – it only adds to the uncertainty

Zdr_{Rx}^{RVP} ***Raw receiver bias***- The difference in power between the horizontal and vertical receiver channel outputs measured at the RVP8 when the AME test signals are injected.

Zdr_{Tx}^{RVP} ***Raw transmitter bias*** - The difference between the horizontal and vertical transmitter powers as measured at the RVP8.

$Zdr_{Tx}^{Cal\_Bias}$ ***Power Sense Offset Bias*** - The difference in loss between the two transmitter measurement paths from the RF Pallet to the IFD.

We assume that the factor 2 multiplying the first two biases is to account for the bias by the "above the coupler parts" on transmission?

The equation implies 6 measurements and the analysis was done using estimates of component errors. Quick look at the table and considering NSSL's proposed calibration

procedure (Zrnic, Melnikov, Carter, and Ivic: Calibrating Differential Reflectivity on the WSR-88D, NSSL Report) we offer the following remarks:

1) It appears that the Contractor did not consult this pertinent reference but the earlier text (Zrnic, Melnikov, and Carter: Calibrating Differential Reflectivity on the WSR-88D) because only the earlier report is listed as reference?

2) The Report Part II suggests a procedure whereby three measurements are made on the receiver side. The procedure hinges on

-splitting the signal generator power into *roughly* equal parts (the exact division is immaterial (it is automatically accounted for)

-the split is permanent (and the two outputs are always connected to the couplers above the LNAs. The switching on and off the generator is done on the common line (before the split) and appropriate matching load in the off position must be included.

3) Initial calibration goes like this

Raw receiver bias Zdr_{Rx}^{RVP}

is obtained (actually a digital number) from the retrace calibration.

Sun check Sun Bias Measurement Zdr^{Sun}

is performed (also digital number).

Raw receiver bias

should be repeated for consistency and to make sure there has been no significant change in gains of the two amplifiers during the sun check measurement.

4) Then the bias referred to the receiver is BR = $Zdr^{Sun} - Zdr_{Rx}^{RVP}$. This bias must be taken out (subtracted) from $Zdr_{Rx}^{RVP}(k)$ where k is the index of the volume scan (every 5 or 10 min). It accounts for all the receiver bias!

If the procedure 2) to 4) is followed than normally three measurements would be required. In case that Zdr_{Rx}^{RVP}(after the sun scan) is not close to the one before, more measurements are needed or a check of the system should be made to establish the reason for this discrepancy. In either case the bias equation would reduce to

$$Zdr_{Bias}(dB) = 2Zdr^{Sun}(dB) - 2Zdr_{Rx}^{Sun}(dB) + Zdr_{Rx}^{Test}(dB) + Zdr_{Tx}(dB) - Zdr_{Tx}^{Cal-Bias}(dB)$$

which has one less term. The second term can be ignored if the measurement of sun is bracketed with the measurement of Zdr_{Rx}^{RVP}. Clearly, one important potential source of error (value of the ratio of the powers H and V going into the respective receivers from the generator) would be eliminated. Therefore the contractor's error estimate is higher than what the errors could be if minor adjustment in receiver calibration is made.

Transmitter calibration is made by measurements and accounting for the difference in the transmitted powers, in the measuring of these, and possibly in the antenna part (accounted via Sun measurement)? This part is also more demanding than what could have been done because of the following arguments.

5) *First Postulate* (based on symmetry principle): The directive gains at H and V polarization are equal – and the beam areal cross sections are equal in size. The shapes are also the same except one is rotated with respect to the other by 90 deg (see Figs. 1, and 2). This is explained as follows.

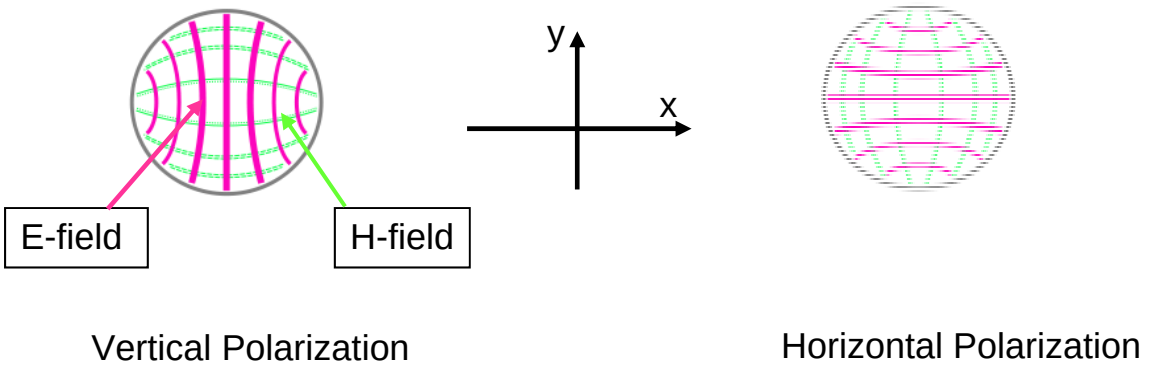

Fig. 1. Distribution of the E and H fields in a circular waveguide. Left: orientation with E primarily vertical. Right: the E field is primarily horizontal and would be obtained by simply rotating by 90 deg the figure on the right. The distribution of fields in the circular waveguide is different from the TE_{11} mode but the same symmetry principle applies.

Let the pattern widths in two orthogonal directions (x,y) for Horizontal polarization be $\theta_{H,x}$ and $\theta_{H,y}$ where h stands for polarization and x, y are the horizontal and vertical coordinates with respect to beam center. For vertical polarization the widths are $\theta_{V,x}$ and $\theta_{V,y}$. This assumption implies an elliptic beam cross section and the pattern described with a product of two Gaussian functions; it is not necessary but helps physical understanding. The differential directivity is defined as

$$\text{Differential Directivity} = \frac{g_h}{g_v} = \frac{\theta_{V,x}\theta_{V,y}}{\theta_{H,x}\theta_{H,y}} = \frac{\text{Beam cross section (V pol)}}{\text{Beam cross section (H pol)}}.$$

The argument in Fig. 1 implies that the differential directivity is 1 i.e., the beam cross sections are the same, but might not be aligned. An exaggerated conceptual representation is in Fig. 2.

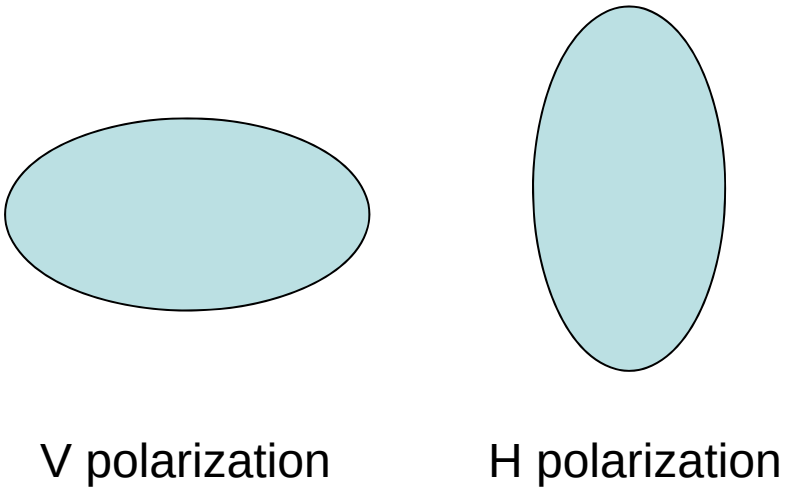

Fig. 2. Beam cross sections for the two orthogonal polarizations.

Which polarization would produce a wider pattern in say the horizontal direction depends on the illumination by the feed. Feed horns are designed to match as well as possible the width of the patterns so the differences are expected to be small. The Symmetry of the patterns and equality of cross sections are expected to be excellent because the precision of the manufacturing process (computer controlled) is very high. Thus we submit that there would be no bias in Z_{DR} due to the antenna. Although the special orientation of the beam cross section can be different the resolution volume sizes (at H and V) polarization would be equal hence there would be no bias if the resolution volumes are filled with uniformly distributed scatterers.

Second Postulate (based on experience): Antenna characteristics are better than what can be inferred from the measurements.

Third Postulate (based on manufacturing capabilities): High power splitters can be manufactured to tolerances better than 0.1 dB. This can be made into a requirement – that is every splitter must be measured by the manufacturer and if faulty it should be rejected.

Fourth postulate (law of differences): If physical reasons dictate two quantities to be almost equal (and measurements generally confirm this) the difference between the two would be much (~order of magnitude) smaller than either one. Case in point concerns the losses from the power splitter to the antenna; these are approximately <0.4 dB.

Thus, if the power splitter were well designed there would have not been a need to calibrate the transmitter path. Assuming equal power would eliminate the possibility of an added uncertainty.

A.4. Recommendation

The most essential part of Z_{DR} calibration is to maintain stability and repeatability. Automatic calibration at end of volume scans should guaranty stability and repeatability, and appears to do that. The observed uncertainty might be due to additional implementation issues and the adjustable power divider in the transmitter chain. Thus, a study is in order. Specifically we should:

- Examine of the details of Z_{DR} calibration as done by the contractor and simplify where possible.
- Measure of the copolar and cross polar patterns on the KOUN.
- Explore use of ground clutter for monitoring stability of Z_{DR}
- Replace the current power splitter with a fixed power splitter and evaluate a simplified procedure.

A.5. References

Barron Services report, 2011: Zdr Calibration Accuracy Analysis, BS-2000-000-107.

Ryzhkov, A.V., and D.S. Zrnic, 1998: Discrimination between rain and snow with a polarimetric radar, *Jour. Appl. Meteor.,* **37,** pp. 1228-1240.

Zrnic, D.S., R.J. Doviak, G. Zhang, and R.V. Ryzhkov, 2010: Bias in differential reflectivity due to cross-coupling through the radiation patterns of polarimetric weather radars. *J. Atmos. Oceanic Technol*., **27**, 1624-1637.

Appendix B. Related Publications

The following papers/presentations relate to the reported material on CLEAN-AP:

Warde, D., S. Torres, and B. Gallardo, 2011: Spectral processing and ground clutter mitigation for dual polarization staggered PRT signals in Doppler weather radars. Preprints, *35th Conf. on Radar Meteor.*, Pittsburg, PA. Amer. Meteor. Soc., Paper 15B.1.

Warde, D., and S. Torres, 2011: Extending the CLEAN-AP filter to staggered PRT signals in Doppler weather radars. Preprints, *27th Conf. on Interactive Information and Processing Systems (IIPS) for Meteorology, Oceanography, and Hydrology,* Seattle, WA, Amer. Meteor. Soc., Paper 9.1.

Warde, D., and S. Torres, 2010: Automated real-time mitigation of ground clutter contamination for Doppler weather radars. Preprints, *6th European Conf. on Radar Meteor. and Hydrology (ERAD)*, Sibiu, Romania, Romanian National Meteorological Administration, Paper P2.10.

Warde, D., and S. Torres, 2010: The CLEAN-AP filter: A novel ground-clutter eliminator for NEXRAD, *Bull. Amer. Meteor. Soc.*, 91, 1173-1174.